U.S. DEPARTMENT OF ENERGY

PNNL-20812

Prepared for the U.S. Department of Energy
under Contract DE-AC05-76RL01830

Marine Animal Alert System

Task 2.1.5.3 – Development of Monitoring Technologies

FY 2011 Progress Report

TJ Carlson
Z Deng
JR Myers
SA Matzner
AE Copping

September 2011

Pacific Northwest
NATIONAL LABORATORY

Proudly Operated by Battelle Since 1965

PACIFIC NORTHWEST NATIONAL LABORATORY
operated by
BATTELLE
for the
UNITED STATES DEPARTMENT OF ENERGY
under Contract DE-AC05-76RL01830

Printed in the United States of America

Available to DOE and DOE contractors from the
Office of Scientific and Technical Information,
P.O. Box 62, Oak Ridge, TN 37831-0062;
ph: (865) 576-8401
fax: (865) 576-5728
email: reports@adonis.osti.gov

Available to the public from the National Technical Information Service,
U.S. Department of Commerce, 5285 Port Royal Rd., Springfield, VA 22161
ph: (800) 553-6847
fax: (703) 605-6900
email: orders@ntis.fedworld.gov
online ordering: http://www.ntis.gov/ordering.htm

This document was printed on recycled paper.
(9/2003)

PNNL-20812

Marine Animal Alert System

Task 2.1.5.3 – Development of Monitoring

FY 2011 Progress Report

TJ Carlson
Z Deng
JR Myers
SA Matzner
AE Copping

September 2011

Prepared for
the U.S. Department of Energy
under Contract DE-AC05-76RL01830

Pacific Northwest National Laboratory
Richland, Washington 99352

Abstract

The Marine Animal Alert System (MAAS) in development by the Pacific Northwest National Laboratory is focused on providing elements of compliance monitoring to support deployment of marine hydrokinetic energy devices. An initial focus is prototype tidal turbines to be deployed in Puget Sound in Washington State. The MAAS will help manage the risk of injury or mortality to marine animals from blade strike or contact with tidal turbines. In particular, development has focused on detection, classification, and localization of listed Southern Resident killer whales within 200 m of prototype turbines using both active and passive acoustic approaches. At the close of FY 2011, a passive acoustic system consisting of a pair of four-element star arrays and parallel processing of eight channels of acoustic receptions has been designed and built. Field tests of the prototype system are scheduled for the fourth quarter of calendar year 2011. Field deployment and testing of the passive acoustic prototype is scheduled for the first quarter of FY 2012. The design of an active acoustic system that could be built using commercially available off-the-shelf components from active acoustic system vendors is also in the final stages of design and specification.

Acronyms and Abbreviations

2D	two-dimensional
COTS	commercial off-the-shelf
dB	decibel
DSP	digital sound processor
ESA	*Endangered Species Act of 1973*
FPGA	field programmable gate array
GPS	Global Positioning System
JSATS	Juvenile Salmonid Acoustic Telemetry System
kHz	kilohertz
µPa	micropascal
µs	microsecond
m	meter
MAAS	Marine Animal Alert System
MHK	marine and hydrokinetic
MHz	megahertz
MMPA	*Marine Mammal Protection Act of 1972*
NMREC	National Marine Renewable Energy Center
NOAA	National Oceanic and Atmospheric Administration
PNNL	Pacific Northwest National Laboratory
SEL	sound exposure level
SPL	sound pressure level
SnoPUD	Snohomish County Public Utility District
SRKW	Southern Resident killer whale
STFT	short-time Fourier transform
TDOA	time difference of arrival

Contents

Figures

1.0 Introduction

Marine and hydrokinetic (MHK) power sources in general and, for this project, tidal power, have been identified as a potential commercial-scale source for sustainable power. A number of tidal power developers and utilities are pursuing deployment of prototype tidal turbines to assess the viability of current designs and sites to provide economically viable power production at commercial scales. Deployment of prototype turbines requires permits from regulatory authorities with the responsibility to protect the safety of marine animals. The most challenging aspect of selecting a site and permitting tidal turbines in U.S. waters is ensuring the safety of marine animals, particularly those under special protection of the *Endangered Species Act of 1973* (ESA) and *the Marine Mammal Protection Act of 1972* (MMPA). The greatest perceived danger to marine animals is from strike by the rotating blades of tidal turbines. When marine mammal species in the vicinity of a proposed MHK project are listed under the ESA, the regulatory mandate allows zero "take," defined as injury, mortality, or harassment of the animals, without an action-specific "no jeopardy" opinion and associated incidental take authorization. National Oceanic and Atmospheric Administration (NOAA) Fisheries has responsibility for enforcing the MMPA and the ESA; NOAA regulators have stated that they will not allow deployment of tidal turbines unless they are assured that listed marine mammals are not at risk. Potential risk to other animals with special protection has not yet been addressed.

Pacific Northwest National Laboratory (PNNL) proposed to develop technology to assist the MHK industry in managing the risk of injury or mortality to animals from blade strike or other direct interaction with MHK devices, using passive and active acoustics. The primary purpose of the Marine Animal Alert System (MAAS) technology is to provide monitoring of animals in the vicinity of the MHK devices; secondarily, the MAAS can assist with mitigating the risk to marine animals.

The initial target application for MAAS development has been focused on monitoring for interaction of the ESA-listed Southern Resident killer whales (SRKWs) in Puget Sound with operating OpenHydro devices proposed for development by the Snohomish County Public Utility District (SnoPUD). Regulatory authorities have taken the position that they will not permit prototype tidal turbines to be deployed unless they are assured that the SRKW will face no risk from blade strike by operating turbines. The MAAS has been developed as a monitoring device to detect and estimate the location of SRKW when they are within 200 m of the prototype tidal turbines and alert turbine operators about the presence of SRKW in proximity to the turbines so that mitigating action may be taken.

Passive acoustics were selected as a means to detect the presence of SRKWs because of the vocal nature of these animals. SRKWs use echolocation to find their food and communicate with one another using a variety of calls. Active acoustics were selected to detect and localize SRKWs within 200 m of tidal turbines when they were not vocalizing and to provide information about other protected but not listed species of marine animals that might approach an operating turbine.

Elements in the strategy for development of the MAAS include

- Establishing performance requirements for both passive and active acoustic system detection and tracking of SRKW, and alerting turbine operators to the presence of SRKW.

- Developing specifications and prototype MAAS system elements to permit MHK project developers, regulators, and stakeholders to evaluate the potential effectiveness of the system in managing risk to the SRKWs.
- Carrying out a validation test of the MAAS in the presence of SRKWs, in waters similar to the proposed SnoPUD deployment site.
- Investigating the availability of commercial off-the-shelf (COTS) acoustic instruments to manage costs and enable deployment of MAAS on commercially deployed MHK devices.
- Working with regulators and stakeholders to ensure that the effectiveness and utility of the MAAS meets siting and permitting requirements to get MHK devices in the water.

Progress has been made in all areas of the MAAS development strategy during FY 2011, the first year of the project. Section 2 of this progress report presents a summary of the status of the passive acoustic portion of the MAAS and the steps remaining to completion of the MAAS. A review of development progress for the active acoustic portion of the MAAS is given in Section 3. The summary in Section 4 presents the steps for completion of the MAAS. Sources cited in this report are listed in Section 5. Technical papers produced during FY 2011 as part of this project are included as Appendices A, B, and C.

2.0 Marine Animal Alert System Passive Acoustic Component Status

The MAAS passive acoustic system consists of the hardware and software that process the output of receiving array hydrophones to obtain the bearing and range to a sound source. The system also includes the software to perform signal processing to complete a two-stage process to distinguish between calls from killer whales and noise.

2.1 System Bearing and Range Estimation

The MAAS passive acoustic system consists of the elements shown in the block diagram of Figure 2.1.

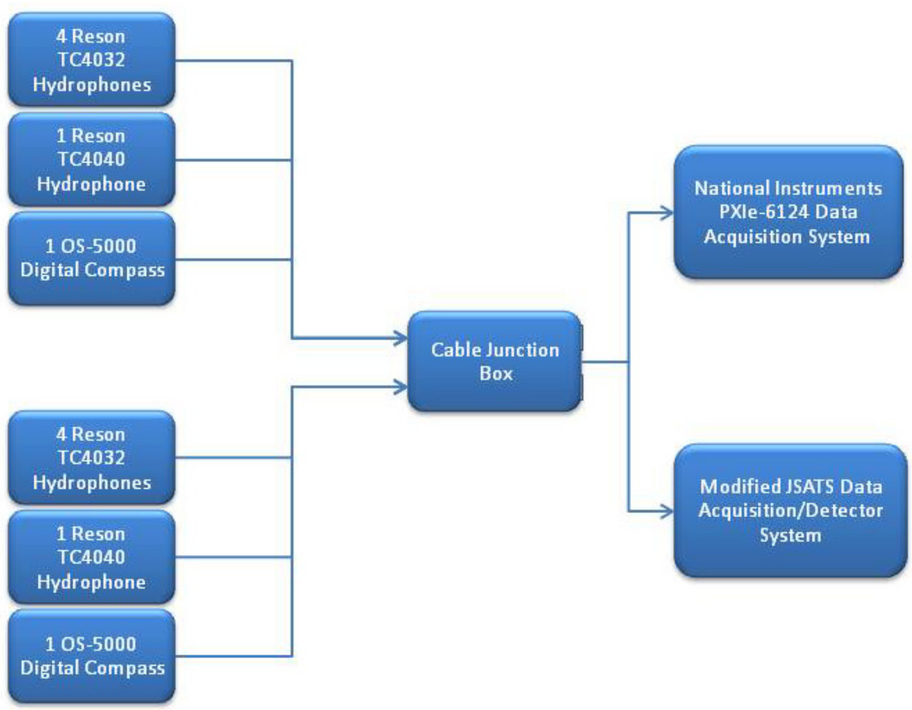

Figure 2.1. Marine Animal Alert System passive acoustic system.

The in water portion of the system is two modified star arrays (Au and Herzing 2003), each consisting of four Reson TC4032 hydrophones. One hydrophone is located in the center of the array with the other three on 2-m-long extensions with 120° separation (Figures 2.2 and 2.3). The two star arrays when deployed will be separated by 20 m. When in use, the two arrays are operated independently but are synchronized to a common clock using a Global Positioning System (GPS) receiver. A bearing to a detected sound source is determined for each array, and the range to the source is determined using the intersection of the two bearings. Figure 2.4 provides additional detail to that of Figure 2.1 for the localization function of the passive acoustic system.

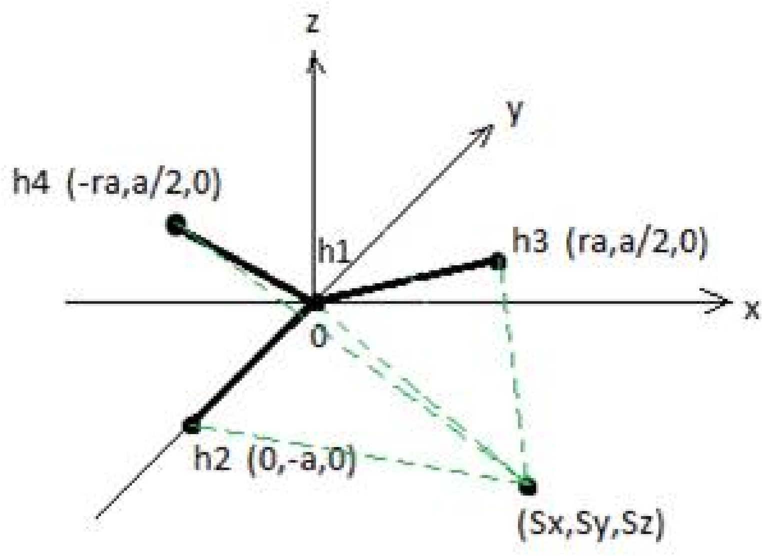

Figure 2.2. Location of the four hydrophones in a star array and their location relative to a sound source located at (Sx, Sy, Sz).

Figure 2.3. A star array mount prior to deployment. When deployed, a hydrophone is attached to the uprights at the center and the end of each of the arms of the mount.

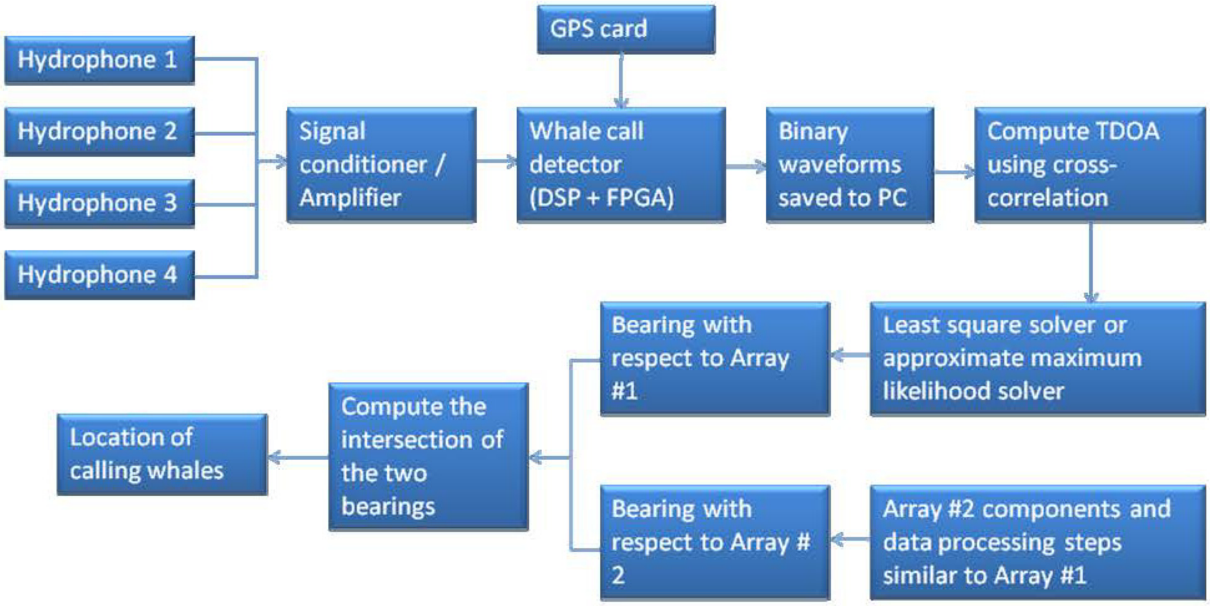

Figure 2.4. Function of the MAAS passive acoustic system to obtain the bearing and range to a vocalizing SRKW.

The four channel receivers for the star arrays are based on four-channel acoustic telemetry receivers developed for the U.S. Army Corps of Engineers (Deng et al. 2011; Weiland et al. 2011). These receivers simultaneously sample the output of the hydrophones in the arrays at a 1-MHz rate and perform a two-step SRKW call detection process in real time, followed by computation of the differences in the time of arrival of whale calls at the elements of the two star arrays. The arrival time differences are manipulated to estimate the bearing to the whales from each array. Finally, the intersection of the two bearing estimates is computed to provide an estimate of the location of the calling whale.

The expected performance of the array for a 20-m separation of the star arrays based on mathematical modeling is as follows:

- Within 200 m of the array baseline, the error of bearing estimates in the *x*–*y* plane (two-dimensional [2D] error) are expected to be within 5°. The error in bearing estimates is largely independent of depth (*z*).
- The detection range and the error in range estimates depend on the time difference of arrival (TDOA) errors of a call at array hydrophones resulting from different types of measurement errors (hydrophone location estimation error, sound of speed estimation error, and time of arrival estimation error).
- •If the combined TDOA error is on the order of 10 µs, the detection range will be up to 200 m with 15-m accuracy in the sound source location estimate. If the combined TDOA error is on the order of 100 µs, the detection range will be about 100 m with 15-m sound source location estimate accuracy.
- The sampling frequency of the MMAS receivers is 1 MHz, and the GPS receiver clock has 0.4-µs accuracy. Therefore, we expect TDOA errors to be on the order of 10 µs.

Overall, the accuracy and precision of the bearing and range estimates system are functions of accurately knowing the spacing orientation of the star arrays and the spacing of the array of hydrophones on each star. The selected spacing of 20 m would permit the arrays to be located within the perimeter of the foundation of the 6-m OpenHydro tidal turbine currently being planned for deployment in Puget Sound.

The prototype MAAS passive acoustic system will be completed in the last calendar quarter of 2011 and deployed in Sequim Bay for evaluation. The performance of the system will be evaluated using a variety of signal types including SRKW calls that were acquired from various sources during the early phases of the project.

2.2 Southern Resident Killer Whale Call Detection and Classification

The requirements for the MAAS passive acoustic system SRKW call detection and classification tasks are particularly rigorous. The objective of the MAAS is to provide tidal turbine operators with information with which they can assess the risk to SRKW within 200 m of continued turbine operation. If the system determines that SRKW are present when they are not (a false detection), the turbine will be shut down needlessly. If the occurrence of false detections is too frequent, testing of the prototype turbines for mechanical function and power production may not be successful.

The MAAS SRKW detection system has two stages (Figure 2.5). In the first stage, an energy detector determines if a sound that may be a SRKW call is present. If a candidate sound is determined to be present, it is captured for the second stage of processing. In the second stage, the candidate sound is processed to determine if it has the characteristics of a SRKW call or is another sound, such as vessel noise, that was not produced by a SRKW.

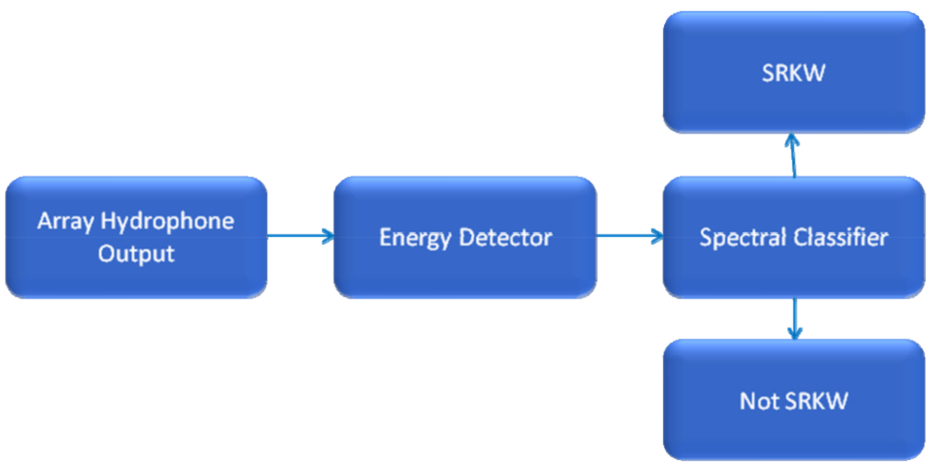

Figure 2.5. Major elements of the detection and classification component of the MAAS passive acoustic system.

The processing flow for the MAAS whale call energy detector, the first of two stages in processing of array hydrophone output to detect and classify SRKW calls, is shown in Figure 2.6. Audio signals enter the detector from star array hydrophones. The signals are filtered to a band that is known to contain most of the energy in killer whale calls, and then the signals are squared. The squared signal from each hydrophone is accumulated if the energy in a sum window of specified length continues to increase. If the signal continues to increase over a set period of time, it is classified as a candidate whale call and saved to storage. Figure 2.7 shows a section of an audio signal received from a hydrophone and the response of the detector to segments within the sample that contain known whale calls. Also shown are audio signal segments that are noise but satisfy detector rules and are identified as candidate whale calls and captured for further processing.

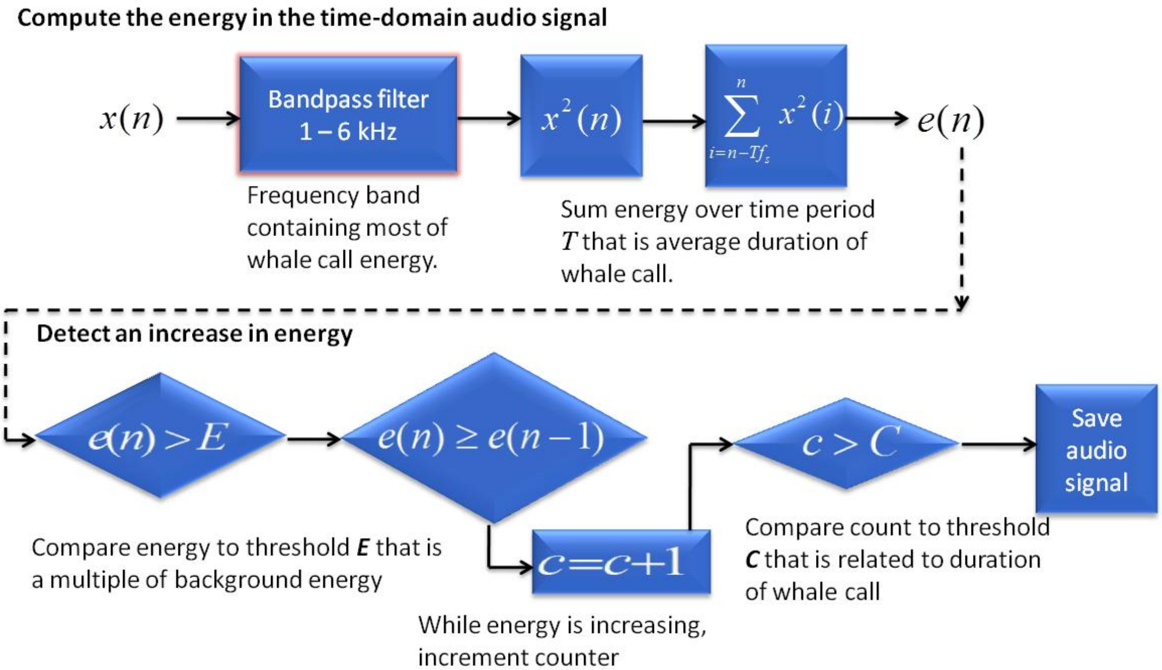

Figure 2.6. Processing flow diagram for the MAAS whale call energy detector.

Segments of star array hydrophone audio signals that are identified as candidate whale calls are further processed to reduce the occurrence of false detections while preserving true detections. The processing flow for the classification stage of the whale call detector is shown in Figure 2.8. The first step in processing a candidate whale call is to obtain a spectrogram. A spectrogram is a plot of the frequency content of a signal over time. The spectrogram is then filtered and statistically processed to remove elements that are not typical of whale calls and converted into a binary image. Image processing techniques are then used to determine if the remaining spectrogram has features that are typical of a whale call. If the answer is yes it is classified as a valid detection.

Figure 2.9 shows a series of spectrograms at three stages in processing in classification of a candidate whale call. The first spectrogram is that recovered by applying a short-term Fourier transform to the candidate whale call audio segment. The second spectrogram is that resulting from applying a 2D low-pass filter to the initial spectrogram. This step preserves the peaks in the spectrogram that contain the most information about the probable source of the audio segment. The final spectrogram is that resulting from a process that subtracts the background noise from the spectral data and converts the spectrogram in to a binary image that can be rapidly processed to complete classification of the candidate signal. A paper prepared for the IEEE OCEANS 2011 conference and presented in September 2011 is included as Appendix A. This paper provides information summarizing development of the whale call detection process described and the results of investigation of whale call detection algorithms developed by others that were investigated during the earlier stages of this project.

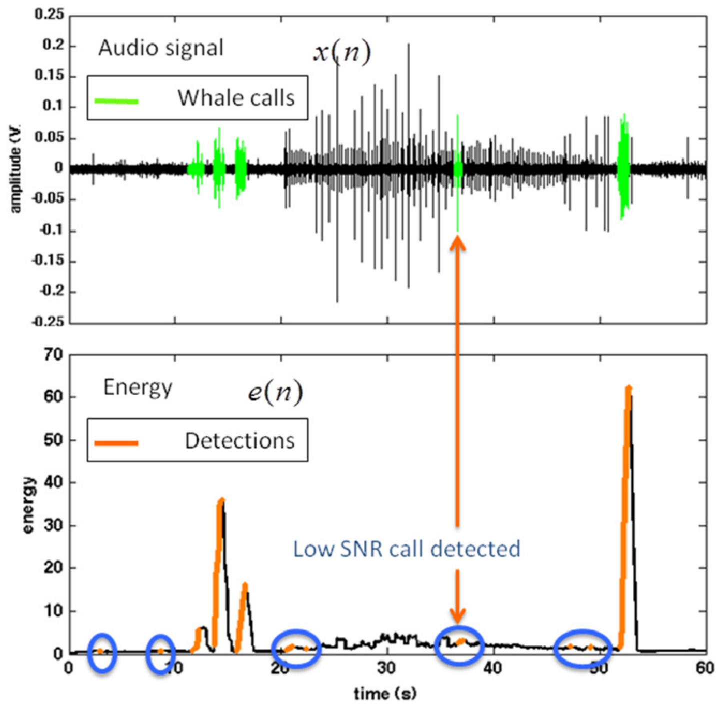

Figure 2.7. Audio signal from a star array hydrophone (upper panel) and corresponding output of the whale call detector (lower panel). Upper panel regions highlighted in green are known whale calls. In the lower panel, orange highlights are segments of the detector output that correspond to the known whale calls. Detector segments circled in blue are segments of the audio signal out of the hydrophone that satisfy the detector rules as whale call candidates.

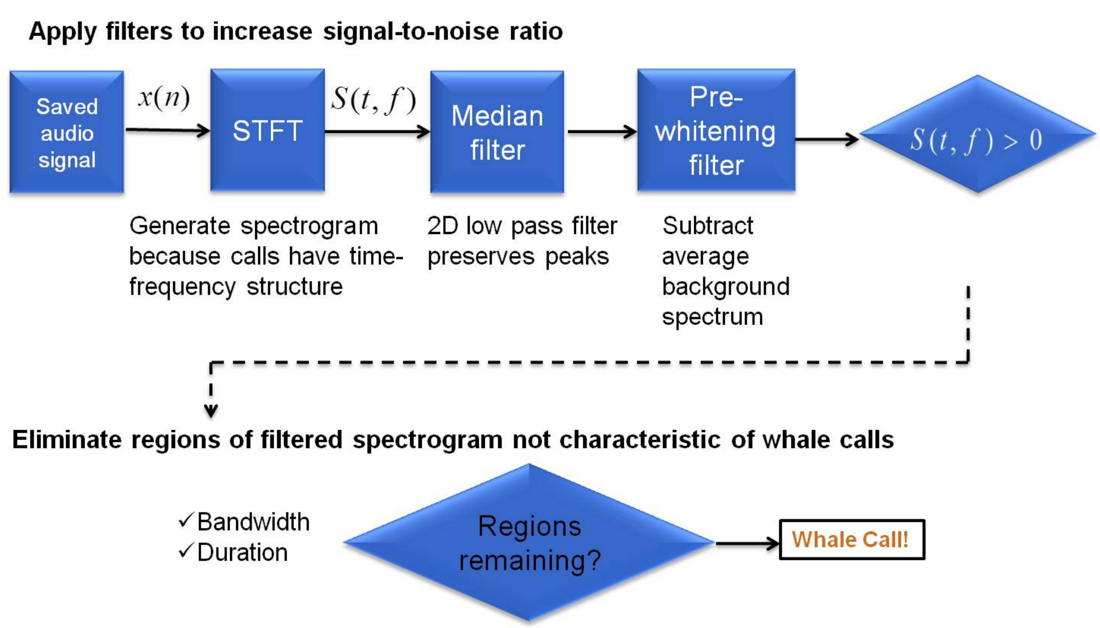

Figure 2.8. Steps in processing a candidate whale call detection to decide if it is a valid whale call detection or not.

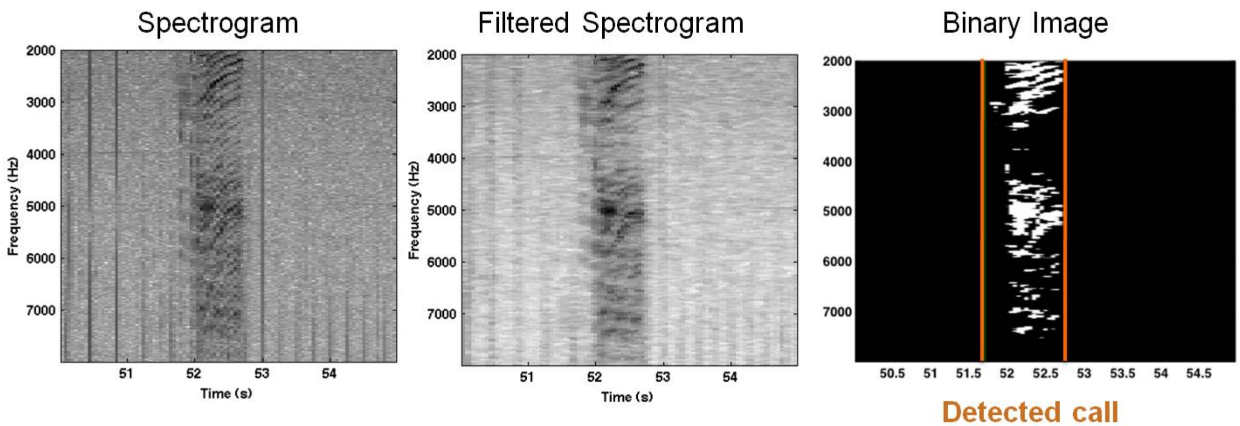

Figure 2.9. Spectrograms illustrating treatment of the spectral information in the whale call candidate signal to prepare the sample for classification.

As of the end of FY 2011, the structure of the two-stage whale call detector, coding of algorithms in MATLAB, and initial evaluation of detector performance have been completed. The remaining steps for completion of the whale call detection section of the MAAS passive acoustic system currently under way are optimization of signal processing algorithms so that they can be implemented in real time, followed by in-field evaluation of real-time performance using playback of recorded SRKW calls.

3.0 Marine Animal Alert System Active Acoustic Component Status

The design of an active acoustic system for SRKW detection had to take into consideration the frequency of operation of candidate sonar systems, the noise environment within the frequency band of operation of the system at the prospective turbine locations, the target strength of SRKW, and development of algorithms and the computing environment for processing multiple channels of active acoustic echo returns. Here we will report the progress to date for sonar operating frequency selection, assessment of the noise at sonar frequencies at prospective tidal turbine locations in Puget Sound, and progress on estimation of the target strength of SRKW. Work has been initiated on echo return processing, but there are no significant results to present at this time.

3.1 Sonar Operating Frequency

The operating frequency of the active acoustic system was selected to be 200 kHz. This frequency of operation for sonar systems in the presence of killer whales and other marine mammals has been accepted by regulatory authorities. The 200-kHz frequency has been accepted because it is above the known frequency range of hearing of marine mammals, including killer whales. Szymanski et al. (1999) developed audiograms for killer whales using both behavioral responses and auditory evoked potential observations. The most sensitive region of hearing for these animals was in the range from 18 to 42 kHz with threshold sound pressure level (SPL) values in the range of approximately 40 dB re 1 μPa. The audiogram shows rapidly decreasing hearing sensitivity from about 80 kHz up to 100 kHz. 100 kHz was the highest frequency at which the whale's hearing was tested. At 100 kHz, the threshold of hearing was observed to be an SPL of approximately 120 dB re 1 μPa. Functionally, given the noise environment in the ocean, the threshold for hearing at 100 kHz is the upper end of the killer whale's hearing range. This is the reason 200 kHz has been identified as an acceptable frequency of operation for active sonar systems that will be used in the presence of killer whales.

Our selection of the 200-kHz frequency and request for permit to deploy an active sonar system in a location known to be frequented by SRKW and other killer whales at this frequency level was contested by state and county permitting authorities at the recommendation of private parties who expressed concern about the use of 200 kHz sonars near killer whales. The concern expressed by the private parties at the base of concerns by the regulatory authorities was that previous experience with sonars operating at this frequency seemed to affect the behavior of exposed killer whales. Given this response, we investigated the frequency content of the pulses generated by the COTS sonar systems we had identified as candidates for the data acquisition portion of the active acoustic portion of MAAS.

The manufacturers of the candidate active acoustic systems were contacted and asked if they would participate in an in-field evaluation of the frequency content of the pulses transmitted by their sonars. An example of a typical result is shown in Figure3.1. Although on the order of 99% of the energy in the transmitted signals below the carrier frequency of 200 kHz was within 50 kHz of the carrier frequency, there was sound within the hearing range of killer whales. Comparison of the level of sound in the sonar pulses measured at a range of 100 m from the sonar transducer with the audiogram of killer whales shows sound levels between 10 and 100 kHz that are on the order of 60 dB ref 1 μPa above the hearing threshold of the whales. Analysis of these data in the context of the noise within the hearing range of killer whales is under way. Initial indications too premature to report in detail here suggest that assessment sonars of the type tested could be heard by killer whales at ranges of about 200 m from the sonar's transducers. Consideration of the acceptability of active sonar as an element of a MAAS in Puget Sound by regulatory authorities and others will be conducted following receipt of our final report on our measurements and analysis.

Appendix B provides a paper prepared for the IEEE OCEANS 2011 conference that contains some additional analysis of the frequency content of active sonar signals.

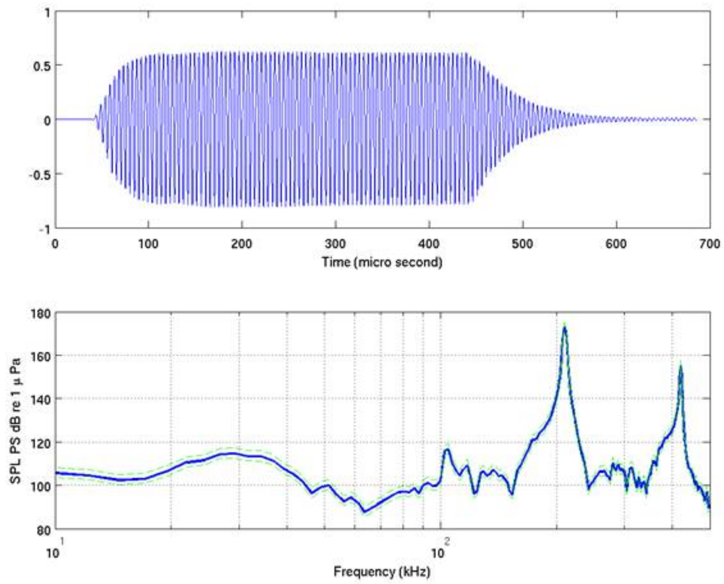

Figure 3.1. Pulse received from an active sonar system at a range of 100 m from the sonar transducer (upper panel) and frequency content of the received signal in terms of sound pressure level (SPL) in decibels referenced to a micropascal (lower panel).

3.2 Assessment of Broadband Noise at a Prospective Tidal Turbine Site in Puget Sound

The background noise over the operating frequency bandwidth of a sonar system affects the ability of the system to detect echoes from targets. No noise data for the operating bandwidth of a 200-kHz sonar were available for Admiralty Inlet. In collaboration with staff from the Northwest National Marine Renewable Energy Center (NMREC) at the University of Washington, PNNL fielded broadband sound measurement equipment at the proposed site for deployment of a prototype tidal turbine in Puget Sound. Analysis of one of the first blocks of acquired data was conducted and is presented in a paper to the IEEE OCEANS 2011 conference (Appendix C). Analysis of all of the noise measurement data acquired at the Puget Sound tidal turbine site is currently under way. This work is being conducted in collaboration with NMREC staff and will be presented in a final project report in FY 2012.

3.3 Estimation of Killer Whale Target Strength

Target strength of the targets of interest is a required measure in design of an active sonar system. It is a measure of the ratio of the sound reflected back from the target toward the sonar transducer to that transmitted by the sonar system that is incident on the target. The target strength of an object such as a killer whale is complex because of the physics of the response of the incident sound to the properties of the body of the whale, the size of the whale, and the aspect of the whale at the instant of ensonification.

We are currently completing work on a model of the target strength of killer whales that is based on measurements of a bottlenose dolphin, a relative of killer whales (which are also dolphins), made by Au (1966). Au made measurements of a trained bottlenose dolphin at 67 kHz. By changing the aspect at which he ensonified the dolphin, he was able to obtain target strength directivity. The target strength directivity Au obtained for his trained dolphin is presented in Figure 3.2. The target strength values shown are relative, not absolute, and are in decibels. Also shown in Figure 3.2 is our initial estimate of the directivity of killer whales. These values were estimated by assuming allometry between dolphin species, particularly in lung volume. Au found that the lungs of the bottlenose dolphin were the major source of backscatter at 67 kHz from the bottlenose dolphin he measured. Additional information on the method used to obtain the killer whale target strength directivity can be found in the paper in Appendix B.

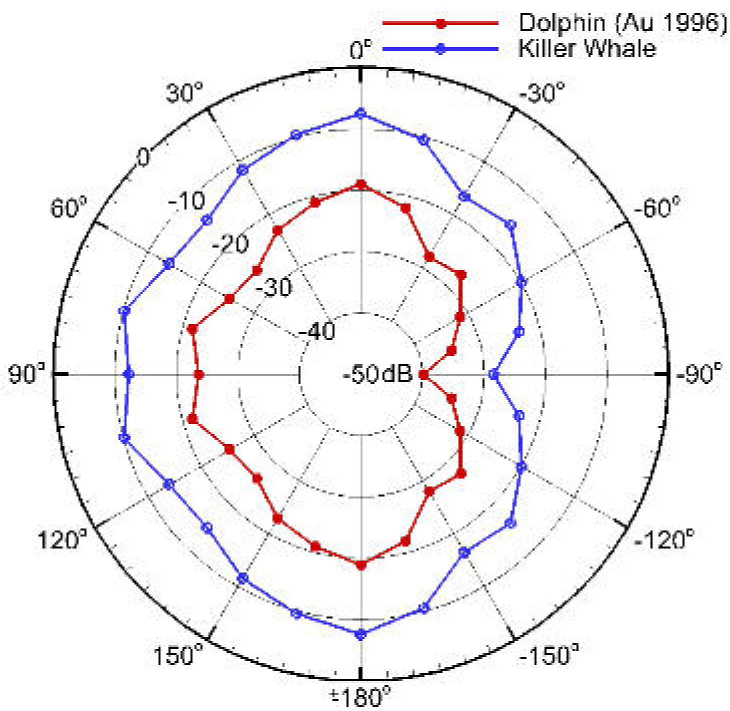

Figure 3.2. Polar plot of the relative target strength in dB for measurements of a bottlenose dolphin by Au (1966) and estimates for the relative target strength of a killer whale.

We are currently extending our killer whale target strength model to include the properties of the killer whale body. We need to estimate the reflectivity of killer whales at sonar operating frequencies of 200 kHz. We have not been able to find any reports in either the peer-reviewed or gray literature of target strength measurements of killer whales at 200 kHz. However, we have obtained a data set of raw acoustic returns obtained from killer whales ensonified at 200 kHz from BioSonics Inc. We are analyzing these data and will use them to assess the validity of the results of our analytical killer whale target strength model. In turn, the killer whale target strength model we derive will be used in conjunction with deployment site noise observations, the operating characteristics of COTS sonar systems, a strategy for system deployment coincident with a tidal turbine, and a model for the behavior of killer whales to estimate the likely operational performance of an active acoustic system for the MAAS.

4.0 Summary

The passive acoustic system portion of the MAAS is in the final stages of development and prototyping. A prototype will be deployed for in-field testing within the fourth quarter of calendar year 2011. In-field testing will assess the performance of the system using a variety of sound sources including playback of recorded SRKW calls. The prototype passive acoustic system and a report of its performance will be completed in 2012.

The active acoustic system portion of the MAAS is in design. The final stages of design require completion of analysis of noise data and validation of a killer whale target strength model. Specifications for an active acoustic system to detect marine animals in the immediate vicinity of tidal power installations will be completed in FY 2012.

5.0 References

Endangered Species Act of 1973. 7 U.S.C. § 136, 16 U.S.C. § 1531.

Marine Mammal Protection Act of 1972. Marine Mammal Protection Act of 1972 (16 U.S.C. 1361-1407, P.L. 92-522, October 21, 1972, 86 Stat. 1027) as amended by P.L. 94-265, April 13, 1976, 90 Stat. 360; P.L. 95-316, July 10, 1978, 92 Stat. 380; P.L. 97-58, October 9, 1981, 95 Stat. 979; P.L. 98-364, July 17, 1984, 98 Stat. 440; P.L. 99-659, November 14, 1986, 100 Stat. 3706; P.L. 100-711, November 23, 1988, 102 Stat. 4755; P.L. 101-627, November 28, 1990, 100 Stat. 4465; P.L. 102-567, October 29, 1992, 106 Stat. 4284; P.L. 103-238, 3, April 30, 1994, 108 Stat. 532; P.L. 105-18, June 12, 1997, 111 Stat. 187; and P.L. 105-42, August 15, 1997, 111 Stat. 1125.

Au WWL. 1996. Acoustic reflectivity of a dolphin. *Journal of the Acoustical Society of America* 99:3844–3848.

Au WWL and DL Herzing. 2003. Echolocation signals of wild Atlantic spotted dolphin (*Stenella frontalis*). *Journal of the Acoustical Society of America* 113(1):598–604.

Deng Z, MA Weiland, T Fu, TA Seim, BL LaMarche, EY Choi, TJ Carlson, and MB Eppard. 2011. A cabled acoustic telemetry system for detecting and tracking juvenile salmon. part 2: three-dimensional tracking. *Sensors* 11(6):5661–5676.

Szymanski MD, DE Bain, K Kiehl, S Pennington, S Wong, and KR Henry. 1999. Killer whale (*Orcinus orca*) hearing: auditory brainstem response and behavioral audiograms. *Journal of the Acoustical Society of America* 106(2):1134–1141.

Weiland MA, Z Deng, TA Seim, BL LaMarche, EY Choi, T Fu, TJ Carlson, AI Thronas, and MB Eppard. 2011. A cabled acoustic telemetry system for detecting and tracking juvenile salmon: part 1. engineering design and instrumentation. *Sensors* 11(6):5645–5660.

Appendix A

Operational Performance Analysis of Passive Acoustic Monitoring for Killer Whales

Operational performance analysis of passive acoustic monitoring for killer whales

Shari Matzner*, Tao Fu†, Huiying Ren†, Z. Daniel Deng†, Yannan Sun†, Thomas Carlson†
*Pacific Northwest National Laboratory
1529 W. Sequim Bay Rd, Sequim, WA 98382
Email: shari.matzner@pnnl.gov
†Pacific Northwest National Laboratory
P.O. Box 999, Richland, WA 99332

***Abstract*—For the planned tidal turbine site in Puget Sound, WA, the main concern is to protect Southern Resident Killer Whales (SRKW) due to their Endangered Species Act status. A passive acoustic monitoring system is proposed because the whales emit vocalizations that can be detected by a passive system. The algorithm for detection is implemented in two stages. The first stage is an energy detector designed to detect candidate signals. The second stage is a spectral classifier that is designed to reduce false alarms. The evaluation presented here of the detection algorithm incoprporates behavioral models of the species of interest, environmental models of noise levels and potential false alarm sources to provide a realistic characterization of expected operational performance.**

I. Introduction

To facilitate the development of offshore sustainable energy, the possible adverse effects on marine life must be understood and addressed. Potential dangers from tidal turbines include collisions with the blades and noise that interferes with a marine animal's ability to forage and navigate. The risk of injury is uncertain because the technology is relatively new and there are only a small number of installations currently in operation around the world. A conservative strategy to prevent harm to marine mammals is to continuously monitor the area around the installation, and to cease operations while marine mammals are present. Continuous monitoring also supports understanding the effects of the installation on mammal behavior.

For the planned tidal turbine site in Puget Sound, WA, the main concern is to protect Southern Resident killer whales (SRKW) due to their Endangered Species Act status. The Southern Residents are a distinct population segment of killer whales (Orcinus orca) found in the coastal waters of Washington state and British Columbia. The population was listed as endangered in 2005 and the size of the population was reported to be 87 whales in 2007 [1]. A passive acoustic monitoring modality is appropriate for these whales because they are known to vocalize often. Their vocalizations include both pulsed calls and echolocation clicks.

This paper describes a proposed passive acoustic detection algorithm and a method for evaluating the operational performance. There are no specific requirements at this time beyond the general requirement that some sort of monitoring system be in place to protect the whales. Therefore, a model based on available behavioral and environmental data was used to determine reasonable performance guidelines; the details of the model are given in the next section. The data used for the evaluation, described in Section III, represented the conditions at the proposed site. In Section IV the proposed algorithm is described and the results of a preliminary evaluation.

II. Performance Model

The objective is to reliably detect the presence of killer whales when they are in the vicinity of the turbine and to minimize false alarms that result in unnecessary shutdowns.. The distance at which the whales must be detected is determined by the time required to effect a turbine shutdown and the speed at which the whales travel. The whales have been observed to travel at speeds of 6.5 to 20.4 kph [2], or 1.8 to 5.7 meters per second. Allowing 60 seconds between detection and turbine shutdown means that the whales must be detected between 108 and 342 meters away.

The probability that when a whale is present it will be detected can be modeled as

$$P_d = \sum_i p(v_i) p(d_i | \text{SNR} \geq X) \qquad (1)$$

where $p(v_i)$ is the probability that a whale is emitting vocalization type i, e.g. a pulsed call or a click, and $p(d_i|\cdot)$ is the probability of detection for the ith type of vocalization for a given signal-to-noise ratio (SNR). The probability of vocalization must be included to accurately assess the performance of a passive system, since detections can occur only if the animals are vocalizing. The minimum SNR was estimated from source levels reported in the literature, the estimated transmission loss over the distance 342 meters and the expected background noise level.

The background noise consists of ambient sounds from sources such as waves and cobble movement, and of noise from ship traffic and small boats. A series of measurements were taken at the proposed site by PNNL and the University of Washington to estimate the background noise levels, which were observed to be between 70 - 80 dB re 1 μPa in the 1 - 5 kHz band. The turbine itself will be a source of noise. The worst case noise level, with the turbine operating at maximum speed and foul weather conditions, is expected to be near 110 dB re 1 μPa in the 1 - 5 kHz band [3]. The source levels for killer whale calls reported in the literature are in the range 160 dB re 1 μPa for calls [4] and 195 - 224 dB re 1 μPa for clicks [5]. Using a conservative spherical spreading model for transmission loss, the SNR at 342 meters was estimated to be

$$\mathrm{SNR}(r = 342) = 160 - 20\log_{10} 342 - 110 = 1 \quad \mathrm{dB} \qquad (2)$$

This represents the estimated worst case SNR when the whales are at least 60 seconds away from the turbine.

As in any detection problem, there is a trade-off between the probability of detection and the false alarm rate. The probability of false alarms generated by specific sources can be estimated using the probability of a source's presence and the probability that it's sound will erroneously trigger the detector. For example, small motorized boats produce narrowband harmonic tones that are similar to those of a pulsed call. At this time, the cost of a false alarm has not been quantified so it is not possible to identify the optimal balance between the risk of missed detections and the probability of false alarms.

III. Dataset for Evaluation

The evaluation dataset consisted of three groups of recordings: whale calls, background noise only, and small boats only. All the data except the small boat sounds were recorded at Lime Kiln State Park on San Juan Island, WA during July and August of 2010. These data were collected by the Beam Reach Marine Science and Sustainability School as part of their educational program. The sensor was a Reson TC4032 and the sampling rate was 192 kHz. The sampled signal was saved to disk once per minute, with new files beginning on the minute.

One set of recordings was made during daylight hours. A human observer, one of the Beam Reach students, would note the presence of whales and begin recording. A second set of recordings were made during the night between 22:00 and 05:00 local time, on five different nights. Audio was recorded continuously during these periods and no human observer was involved. The background noise only data were selected from the night recordings when no whales were present. A total of six hours of recording was used for this dataset. The small boat sounds were recorded at PNNL's Marine Sciences Laboratory on Sequim Bay using a Bentos AQ-1 hydrophone and the sampling rate was 10 kHz. The boats were between 80 and 100 meters away at the closest point of approach to the sensor.

. For the recordings when whales were present, annotations were made noting the start and end times of calls and clicks within a subset of the files. An attempt was made to assign a type to the calls. The annotations were made manually using the Audacity software program to simultaneously listen to the audio and visualize the spectrogram. For the daytime recordings, a selection of files based on the observer logs were annotated; the selection was motivated by a particular research interest and do not include all the calls during a period when the whales were present. These annotations were verified by a second researcher, who checked a random sample of 25% of the total annotated files. For the night recordings, the times when whales were present were determined by an independent monitoring system, the OrcaSound Network, that uses a combination of automated signal detection and human listeners to track SRKW movements. The recordings from these times were then annotated systematically by examining each minute of recording in sequence until a pre-defined number of calls and clicks had been identified. A total of 991 calls and 121 click trains were annotated.

The purpose of dividing the data into the three sets was to evaluate the detection system under three different conditions: whales are nearby, no whales or boats are nearby, and boats are nearby. The whale call recordings were used to evaluate the probability of detecting the presence of whales. When the whales are present, there are multiple animals vocalizing and so there are many overlapping calls and a high density of calls per minute. The observer annotations may not include all the calls in a particular recording, so these recordings could not be used to reliably measure false alarm rates. The recordings of background noise only and of small boats are known to contain no whale calls, so these recordings were used to analyze the characteristics of false positive detections.

IV. Detection Approach

The detection system consists of two stages. The first stage is an energy detector that is designed to detect any signal that is not background noise. The second stage is a spectral classifier designed to specifically detect killer whale vocalizations. This two-stage approach is similar to that used by Erbe and King [6] for detecting and classifying the vocalizations of different marine mammals. The energy detector can be implemented efficiently in firmware and reduces the amount of data that must be processed by the second stage detector. The role of the second stage detector is to reduce the number of false alarms.

A. Energy Detector

The energy detector used here was originally developed as part of the Juvenile Salmon Acoustic Telemetry System (JSATS) to track juvenile salmon passing through hydroelectric dams in the Columbia River Basin [7], [8], [9], [10]. This energy detector assumes that the background noise amplitude is Gaussian with zero mean. It is suitable to determine the presence of a signal without knowing the details of the signal [11]. Like other traditional energy detectors, the JSATS energy detector consists of three parts: a noise pre-filter, a squaring function and an integrator [11], [10], [8]. The noise pre-filter is a band-pass filter, which limits the bandwidth of the input signal and removes noise that is out of the signal frequency band; the squaring function calculates the square of the signal; the integrator calculates the sum of the squared signal over a time interval T. The output is an energy signal

$$E(t) = \sum_{i=t-T}^{t} (x(i))^2 \qquad (3)$$

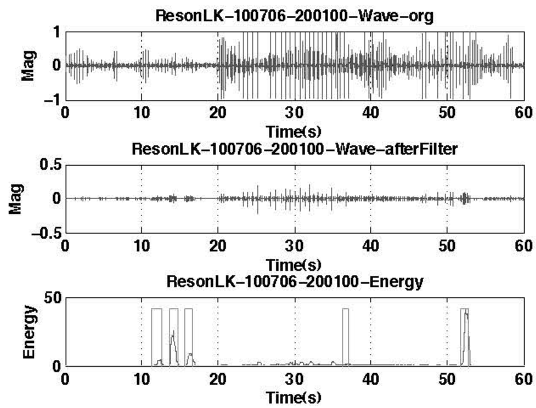

Fig. 1. Time-domain raw signal (top), bandpass filtered signal (middle), energy signal (bottom). The rectangles on the bottom plot indicate the start and end times of calls. The call energy varies which could be due to multiple whales vocalizing at different distances from the sensor.

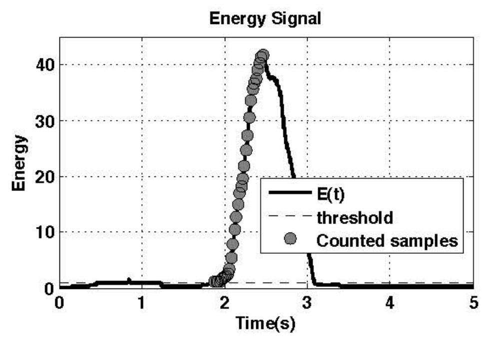

Fig. 2. Example energy signal. The marks indicate the samples that are greater than the first threshold and that are monotonically increasing. In this example, the count is 30 samples.

An example of the raw signal, filtered signal and energy signal for one recording is shown in Figure 1.

The resulting energy signal is decimated and compared to two thresholds. The first threshold is a multiple of the current median energy level. Any samples with an energy level that is less than the first threshold are considered background noise. The number of samples with an energy level above the first threshold and with monotonically increasing energy are counted. When the count exceeds the second threshold, then this part of the signal is considered a signal of interest and the packet that includes these samples is saved for second stage processing. An example energy signal is shown in Figure 2 with the samples marked that trigger a detection.

The parameters of the energy detector are summarized in Table I. The frequency band was selected based on an analysis of the data that determined this band contains a significant portion of call energy for most calls. The integration time and packet size were selected based on an analysis of the duration of the calls in the dataset. Figure 3 shows the cumulative distribution function (CDF) of the duration of the annotated

TABLE I
ENERGY DETECTOR PARAMETERS

Parameter	Value	Description
F_1, F_2	1000, 5000 Hz	Bandpass filter limits
T	0.4 s	Integration window length
P	5 s	Packet length for processing
M	1.2 (unitless)	multiplier for energy threshold
δt	0.02 s	sample interval of energy signal (decimated)
N	5 samples	count threshold

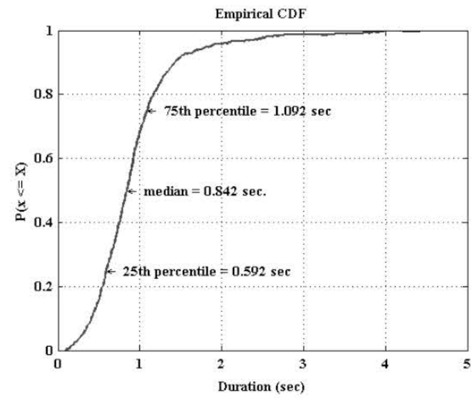

Fig. 3. Killer whale call duration.

calls. The integration interval was chosen to be about half the median duration of the calls and the packet size was chosen to be the 99 percentile call duration. The values for the other parameters were arrived at by analyzing the detection rate versus the false alarm rate using different values, and selecting the value that minimized false alarms while maintaining a detection rate of 95% or better for calls with SNR $>$ 1 dB and a detection rate of 98% for calls with SNR $>$ 5 dB.

B. Spectral Classifier

The pulsed calls of killer whales are characterized by a pattern of narrowband tones that are easily recognized in a spectrogram (see Figure 4). Various methods have been developed for detecting and extracting narrowband signals from spectrograms [12]. The vocal repertoire of southern resident killer whales is comprised of over 30 different distinct call types [5], which makes a template matching approach such as that proposed by Mellinger and Clark for bowhead whale songs [13] impractical. In the context of monitoring for killer whales in Admirality inlet, where mistaking a pulsed call from another species is not a concern, it is sufficient to detect narrowband signals in the spectrogram. The implementation evaluated here is the one used by the PAMGUARD software program for its Whistle and Moan Detector.

PAMGUARD is an open source software program that was developed for the International Association of Oil and Gas Producers(OGP) to monitor for marine mammals during offshore operations (www.pamguard.org, [14]). PAMGUARD has a modular design that allows different detectors to be selected by the user. The Whistle and Moan Detector (WMD)

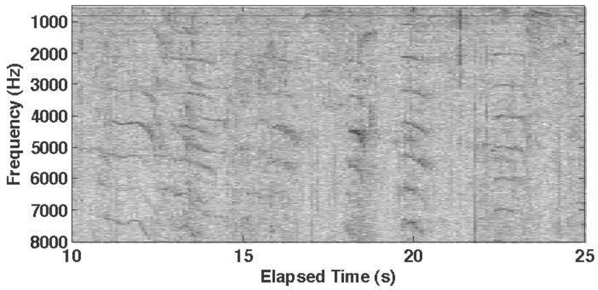

Fig. 4. Spectrogram with killer whale calls.

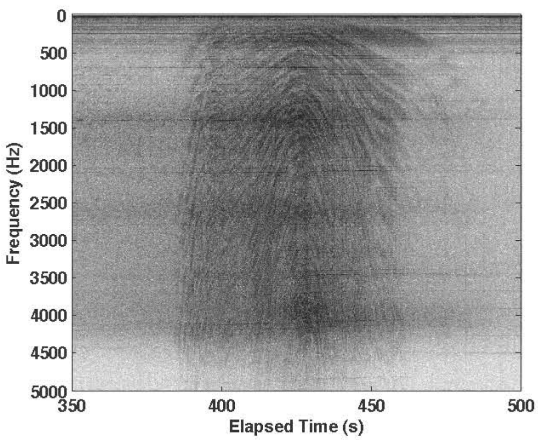

Fig. 5. Spectrogram with small power boat.

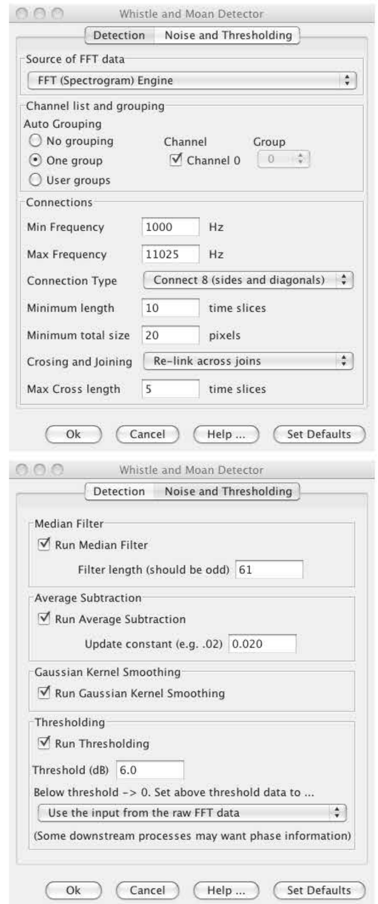

Fig. 6. PAMGUARD settings used for evaluation.

is appropriate for killer whale calls. This detector identifies narrowband signals in the spectrogram using image processing techniques and reports each signal that is detected. Therefore, a single pulsed call generates multiple detections when multiple harmonics are present. Each detection is characterized by a start and end time, the lowest and highest frequencies of the narrowband signal, and the maximum amplitude.

The WMD was evaluated using the four groups of recordings. The settings used for the detector are shown in Figure 6. The probability of detection for the annotated whale calls was 83%, i.e., 83% of the calls generated at least one detection. The six hours of background noise only recordings generated 477 detections, averaging 1.3 detections per minute. There were detections for 187 out of the 360 total minutes. The boat recordings, which included 24 boat signals and totaled 140 minutes of audio, generated 1276 detections. An example boat signal is shown in Figure 5. Boat signals are recognized by the V-shaped broadband noise superimposed with very narrowband tones.

The characteristics of the reported detections for each of the three groups of recordings were compared to determine features for distinguishing whale calls from other sources. Four characteristics of the detected signals were examined: the duration, the maximum amplitude, the maximum frequency, and the bandwidth. The probability distribution function (pdf) of each characteristic was estimated for each group of recordings using a histogram with 20 bins. The pdf plots are shown in Figures 7, 8,9 and 10.

The results indicate a set of rules that could be applied to the detected narrowband signals to classify the signal as a whale call. For example, false alarms due to boats could be eliminated by comparing the duration of a detected narrowband signal to a threshold of one second. The background noise generated detections that were shorter in duration than the true positives. The amplitude of the whale calls and the boats was similar; the amplitude of the background noise detections was lower, in general, but the pdfs of the whale calls and background noise detections overlap. Both detections due to boats and background noise tended to occur at frequencies less than 2 kHz. The settings for the WMD specified the band of interest from 1 kHz to 11.025 kHz and whale calls were detected over this entire band. The boat signals had a very narrow bandwidth compared with the whale calls. The whale calls tend to exhibit a change in frequency over time; a good

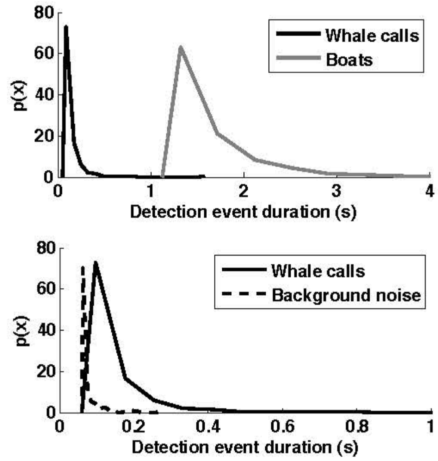

Fig. 7. Empirical pdf of the duration of detections reported for each group of recordings.

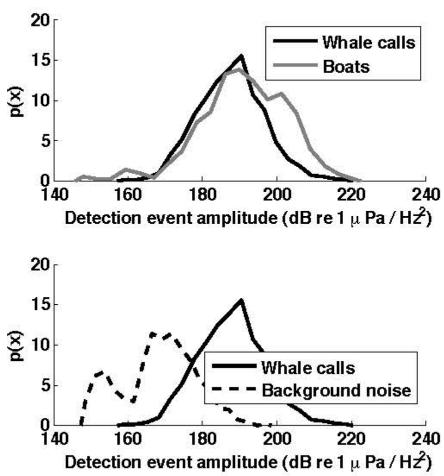

Fig. 8. Empirical pdf of the amplitude of detected narrowband signals for each group of recordings.

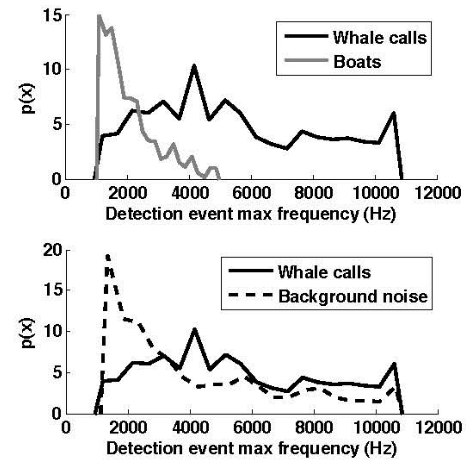

Fig. 9. Empirical pdf of the maximum frequency of detected narrowband signals for each group of recordings.

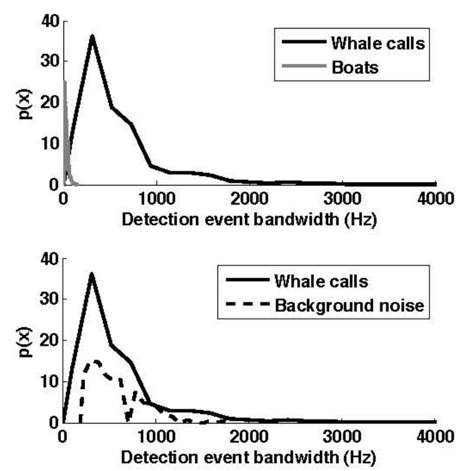

Fig. 10. Empirical pdf of the bandwidth of detected narrowband signals for each group of recordings.

example is the first call visible in the spectrogram in Figure 4.

V. Discussion

The two-stage detection approach presented here addresses two of the general performance requirements for a monitoring system. The system must operate in real-time in order to report detections with enough lead time for the turbine to be safely shutdown. The energy detector supports this goal. It's effectiveness for real-time detection of signals has been proven in the JSATS program. The parameters were tuned to detect the pulsed calls of killer whales so that the probability of detection was 95% with a SNR $\geq$ 1 dB. This represents the probability of detection of individual calls. A more meaningful measure is the likelihood of detecting the presence of whales. This measure can be inferred from the probability of detecting individual calls, the rate at which the whales vocalize, and the number of whales likely to be present. The Southern Residents travel in pods, and there are three pods currently active which are referred to as J, K and L. The sizes of these pods fluctuate but a 2007 estimate put them at 25, 19 and 43 respectively. The rate at which the whales vocalize depends on their behavior; four distinct behaviors are defined as foraging, traveling, socializing and resting. In Ford's 1989 study, he observed that the whales vocalize most frequently (between 15 and 50 calls per minute for the entire group) during foraging and traveling [2]. This finding agrees with the rate of calls in the Lime Kiln data. However, it has also been observed that small sub-groups often forage in silence.

The second general requirement for a monitoring system is to minimize false alarms to avoid unnecessary shutdowns that reduce the overall effectiveness of the turbine. The second stage spectral classifier can accomplish this based on the pdfs of the spectral features of the three different classes – whale calls, boats and background noise. The pdfs suggest that whale calls could be distinguished from boats based on the signal duration and the bandwidth. The whale calls could be distinguished from background noise using the amplitude, frequency and duration of the signal although there is more overlap in the range of these features for the two classes.

The results of this preliminary evaluation will inform further development of the proposed approach into a working prototype.

ACKNOWLEDGMENT

This work was funded by the U.S. Department of Energy Office of Energy Efficiency and Renewable Energy (EERE) Wind and Water Power Program.

The authors would like to thank their collaborators Jason Wood and Dominic Tollit at the Sea Mammal Research Unit (SMRU) for providing the annotated data and for sharing valuable knowledge about Southern Resident behaviors.

REFERENCES

[1] N. M. F. Service, *Recovery Plan for Southern Resident Killer Whales (Orcinus orca).* Northwest Region, Seattle, 2008.

[2] J. K. B. Ford, "Acoustic behaviour of resident killer whales (Orcinus orca) off Vancouver Island, British Columbia," *Canadian Journal of Zoology*, vol. 67, pp. 727–745, 1989.

[3] B. Polagye, C. Bassett, and J. Thomson, "Estimated received noise levels for marine mammals from OpenHydro turbines in Admirality Inlet, Washington," Northwest National Marine Renewable Energy Center, Tech. Rep., 2011.

[4] R. Riesch, J. K. B. Ford, and F. Thomsen, "Whistle sequences in wild killer whales (orcinus orca)," *Journal of the Acoustical Society of America*, vol. 124, no. Compendex, pp. 1822–1829, 2008.

[5] J. K. B. Ford, "Vocal traditions among resident killer whales (Orcinus orca) in coastal waters of British Columbia," *Canadian Journal of Zoology*, vol. 69, pp. 1454–1483, 1991.

[6] C. Erbe and A. R. King, "Automatic detection of marine mammals using information entropy," *Journal of the Acoustical Society of America*, vol. 124, no. Compendex, pp. 2833–2840, 2008.

[7] G. A. McMichael, M. B. Eppard, T. J. Carlson, J. A. Carter, B. D. Ebberts, R. S. Brown, M. Weiland, G. R. Ploskey, R. A. Harnish, and Z. D. Deng, "The Juvenile Salmon Acoustic Telemetry System: A new tool," *Fisheries*, vol. 35, no. 1, pp. 9–22, 2010.

[8] M. A. Weiland, Z. Deng, T. A. Seim, B. L. LaMarche, E. Y. Choi, T. Fu, T. J. Carlson, A. I. Thronas, and M. B. Eppard, "A cabled acoustic telemetry system for detecting and tracking juvenile salmon: Part 1. engineering design and instrumentation," *Sensors*, vol. 11, no. 6, pp. 5645–5660, 2011.

[9] Z. Deng, M. A. Weiland, T. J. Carlson, and M. B. Eppard, "Design and instrumentation of a measurement and calibration system for an acoustic telemetry system," *Sensors*, vol. 10, pp. 3090–3099, 2010.

[10] Z. Deng, M. A. Weiland, T. Fu, T. A. Seim, B. L. LaMarche, E. Y. Choi, T. J. Carlson, and M. B. Eppard, "A cabled acoustic telemetry system for detecting and tracking juvenile salmon. part 2: Three-dimensional tracking," *Sensors*, vol. 11, no. 6, pp. 5661–5676, 2011.

[11] H. Urkowitz, "Energy detection of unknown deterministic signals," *Proceedings of the IEEE*, vol. 55, no. 4, 1967.

[12] T. A. Lampert and S. E. O'Keefe, "A survey of spectrogram track detection algorithms," *Applied Acoustics*, vol. 71, pp. 87–100, 2010.

[13] D. K. Mellinger and C. W. Clark, "Recognizing transient low-frequency whale sounds by spectrogram correlation," *Journal of the Acoustical Society of America*, vol. 107, no. Copyright 2000, IEE, pp. 3518–29, 2000.

[14] D. Gillespie, J. Gordon, and R. Mchugh, "PAMGUARD: Semi-automated, open source software for real-time acoustic detection and localization of cetaceans," *Proceedings of the Institute of Acoustics*, vol. 30, no. 5, 2008.

Appendix B

Design and Operation Specifications of an Active Monitoring System for Detecting Southern Resident Killer Whales

Design and Operation Specifications of an Active Monitoring System for Detecting Southern Resident Killer Whales

Z. Daniel Deng*, Thomas J. Carlson, Jinshan Xu, Jayson Martinez,
Mark A. Weiland, Robert P. Mueller, Joshua R. Myers, Mark E. Jones
Pacific Northwest National Laboratory
Richland, Washington, USA
* e-mail: zhiqun.deng@pnnl.gov

Abstract—**Before final approval is given to the Snohomish County Public Utility District No. 1 for deploying the first tidal power devices in the United States in an open water environment, a system to manage the potential risk of injury to killer whales due to collision with moving turbine blades must be demonstrated. The Pacific Northwest National Laboratory (PNNL) is tasked with establishing the performance requirements for, constructing, and testing a prototype marine animal alert system for triggering temporary turbine shutdown when there is risk of collision with a killer whale. To develop a system that relies on active sonar two critical areas must be investigated—the target strength of killer whales and the frequency content of commercially available active sonar units. PNNL studied three target strength models: a simple model, the Fourier matching model, and the Kirchoff-ray mode model. Using target strength measurements of bottlenose dolphins obtained by previous researchers and assuming killer whales share similar morphology and structure, PNNL extrapolated the target strength of an adult killer whale 7.5 m in length at a frequency of 67 kHz. To study the frequency content of a commercially available sonar unit, direct measurements of the signal transmitted by the sonar head were obtained by using a hydrophone connected to a data acquisition system in both laboratory and field conditions. The measurements revealed a secondary frequency component at 90 kHz in addition to the primary frequency of 200 kHz. Preliminary results show that the amplitude of the 90-kHz frequency component is above the hearing threshold of killer whales but below the threshold for potential injuries.**

Keywords-underwater acoustics; active acoustic monitoring; sound propagation; Tidal power

I. Introduction

The rapid growth in deployment of marine and hydrokinetic energy devices on a national scale requires extended testing of devices in open water environments to refine estimates of total life-cycle costs and to quantify and mitigate environmental consequences of operation. No tidal power generating devices are currently deployed in the United States in open water environments. A Federal Energy Regulatory Commission preliminary permit has been granted to Snohomish County Public Utility District No. 1 for deploying two tidal power devices built by OpenHydro at a site in Admiralty Inlet in Washington's Puget Sound, for the purpose of studying their long term operation. A primary criterion for final approval is management of the risk of injury to killer whales, as mandated under the Endangered Species Act and the Marine Mammal Protection Act, due to collision with moving turbine blades. Pacific Northwest National Laboratory (PNNL) researchers are establishing performance requirements for, constructing, and testing a prototype marine mammal alert system (MMAS) for killer whale detection, tracking, and alerting that links to a tidal turbine and triggers its temporary shutdown when there is risk of collision. Both passive and active monitoring systems are being considered for the MMAS. The passive monitoring system is being developed by modifying an energy-based juvenile salmon acoustic telemetry system [1-3]. Several commercially available sonars are being evaluated for the active monitoring system. This paper describes preliminary results of the PNNL efforts to model the target strength of killer whales and evaluate the frequency content of a commercially available sonar. Both tasks are critical to the design and expected performance of the active monitoring system.

II. Target Strength Modeling

The acoustic target reflects a portion of the intercepted energy in the directions of the receivers. The measure of the reflected energy is defined as the decibel level of the reflected intensity in the receiver direction relative to the incident intensity, measured 1 m from the effective target center. To classify targets as the killer whale of concern, the animals' target strength must be modeled as a function of acoustic wave incident angle and depth to design and implement an active monitoring system. In general, the target strength of an acoustic object is a function of geometry, size, acoustic impedance, and frequency of the incident signal. The target strength of simple geometric shapes, assumed with large impedance mismatch, can be derived analytically. However, the target strength of

This study is funded by the Wind and Water Power Program of the U.S. Department of Energy Office of Energy Efficiency and Renewable Energy.

more complicated structures is best determined experimentally or through semi-analytical and numerical simulation. In the following, after a brief review of three different target strength modeling approaches for marine biology acoustic research, we will introduce our approach and results of the target strength modeling for a killer whale, based primarily on the target strength modeling of a bottlenose dolphin [4].

A. Models

1) Love Model: The first attempt to model the target strength of fish was made by [5]. This empirical model was developed by combining the nondimensionalized results from different sources. It also assumes the animal can be represented by an air-filled sphere. This method is acceptable only for frequencies below 20 kHz and when the animal is close to the surface so the lungs are fully inflated. The equation is fairly simple to apply:

$$TS(f) = 22.8 * \log(L) - 2.8 * \log(\lambda) - 22.1 \quad (1)$$

where L is the length of the animal in meters and λ is the wavelength in meters but with no dependence on orientation. Reference [4] measured the target strength of a bottlenose dolphin and then made a comparison with the calculated values. He showed that the measured broadside values were close to those predicted by the Love equation [5] at 23 kHz but progressively dropped at higher frequencies to be 12 dB (200%) lower at 80 kHz.

2) Fourier Matching Model: The Fourier matching model (FMM) [6] is a semi-analytical technique based on the recovery of the solution for irregular three-dimensional (3D) bodies from solutions of the Helmholtz equation on separable geometries via conformal mapping. This formula is based on the solution of two-dimensional conformal mapping approach to scattering by an infinitely long cylinder [7], and extended to the scattering from finite-length bodies. It involves the conformal mapping of the scatterer surface, which can be irregular, to a new coordinate system in which the locus of points describing the radial coordinate as a constant coincides with the scatterer surface. Application of this FMM method to predict acoustic scattering from high-resolution representations of the swimbladder alone of the alewife, a swim bladder fish was first implemented by Reeder [8] and compared with its experimental target strength measurements. Although the comparison shows FMM consistently predicts target strengths lower than the data by about 3-5 dB, which could be due to the fact that only the swimbladder is taken into account, the model and data agree with each other in the general structure of the target strength as a function of orientation.

3) Kirchoff-Ray Mode Model: The Kirchoff-ray mode (KRM) model [9-13] predicts the back scattering from a fish by modelling the fish approximately: a contiguous set of fluid-filled cylindrical elements representing the fish body surround a set of gas-filled cylindrical elements representing the swim bladder. Those cylindrical elements are constructed from the digitized shape of the fish body and swimbladder. The backscattering from each cylindrical element is estimated using a low-mode cylinder solution in low ka region (where k is the acoustic wave number and a is the cylindrical radius of the elements), and a Kirchhoff-ray approximation for high ka region. Backscattering cross-sections from each finite cylinder are summed coherently to estimate the target strength.

The KRM model can be applied with the exact shape of the animal's morphology, which is desirable because the resulting approximation is more realistic and provides better accuracy over models based on simple geometric shapes, especially in the geometric scattering region (high ka). For any digitized animal body shape, the KRM model can be used to estimate backscattering as a function of fish length, wavelength (i.e., speed of sound in water/acoustic frequency), and fish tilting. Results from the model can be applied to the swim bladder, body, or the whole fish to illustrate the contribution of the body parts to the total backscatter. For marine mammals such as dolphin and whales with large ka (high frequency and large size), the advanced target strength modeling is more applicable as long as the animal's morphology is available.

B. Approach and Result

Reference [4] performed high-resolution measurements of acoustic reflectivity of a female bottlenose dolphin at 67 kHz frequency as a function of frequency at broadside aspect, and target strength (TS) as a function of incident angle. Our approach was based on his results. We assumed that a whale and a dolphin differ only in lung dimensions, which usually cause the largest reflections. The different TS of lungs from a whale and a dolphin could be assumed to be approximately equal to the difference in TS from two different sizes of a sphere or ellipsoid, which already have analytical solutions. The lung size of a killer whale could be estimated by assuming it shares the same lung-to-body ratio as a dolphin.

In [4], a well-trained female dolphin weighing 126 kg and measuring 2.2 m in length was measured for its acoustic reflectivity. Three different signals were used to measure the animal's TS (two frequency-modulated pulses and a broadband click with a peak frequency of 67 kHz). The final result, averaged from echoes of 20 pings recorded for each angle or section, is shown in Fig. 1 with the solid blue curve [4]. The ratio of the lung size to the full body length of this dolphin is about 0.286. Assuming that dolphins and killer whales share a similar morphological structure and differ only in terms of lung dimensions, a 7.5-m killer whale (mature female) would have a lung size of about 2.143 m. The difference in TS from a 0.6-m-diameter sphere and 2.143-m-diameter sphere is about 10.77 dB [14].

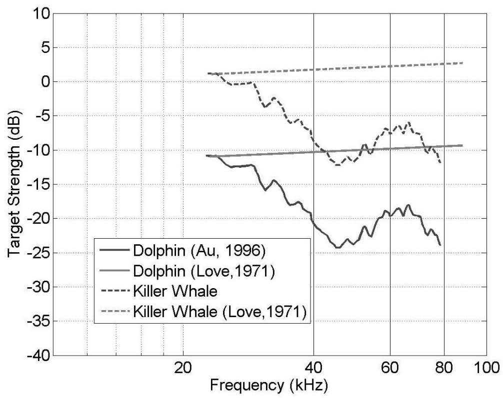

Figure 1. Target strength at broadside aspect as function of frequency [4].

Based on the measured TS as function of frequency of the dolphin at broadside aspect, the TS at broadside aspect as function of frequency for a killer whale could be obtained as shown with the dashed blue curve in Fig. 1. The relative TS with respect to azimuth should be roughly similar to the polar pattern in [4] (Fig. 2).

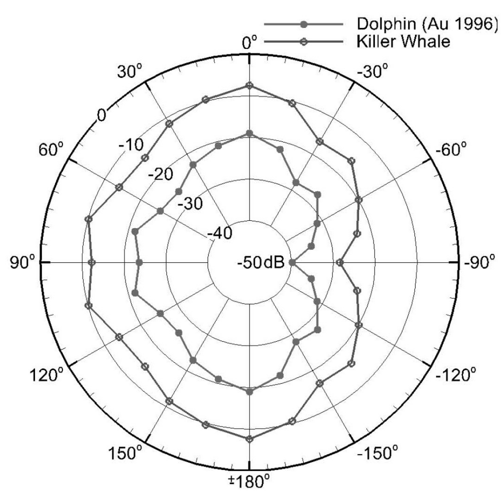

Figure 2. Polar plot of target strength of killer whale at frequency of 67 kHz. Red curve is the target strength of bottle-nose dolphin measured by [4].

The TS of an adult killer whale 7.5 m in length at a frequency of 67 kHz is approximately −8 dB at the broadside aspect, and −28 dB from the tail-on aspect, based on the 10.77 dB translation factor described above. This result is applicable for 7.5-m killer whales swimming close to the surface; however, the TS of aquatic mammals varies with water depth. The variation in TS as a function of depth could be estimated based on the assumption that the lung volume would decrease by 50% for each doubling of hydrostatic pressure [15]. The TS of killer whales at higher frequencies such as 200 kHz can be estimated based on the plane wave reflection coefficient as a function of frequency of a three-layer model (skin, blubber layer, and lung) of the whale [16]. We are investigating these depth-based TS variations further; results will be presented in future venues.

III. Frequency Content Analysis of Active Sonar System

It is critical to determine the design and operating specifications for an active acoustic system that would not transmit energy within the hearing range of killer whales at levels detectable by these animals above ambient noise levels. For a sonar operating at a 200 kHz transmitting frequency, the source level required for a 200-m detection range is approximately 210 dB re 1 μPa at 1 m. Because of the short duration for the transmission of high-power pulses and the sensitive hearing of killer whales within the 1- to 100-kHz range [17], potential energy leakage may occur in the low-frequency range that killer whales can hear. A commercial 200-kHz echo sounder (Model SM 2000 multibeam imaging sonar, Kongsberg-Mesotech Ltd., Vancouver, British Columbia, Canada) was evaluated under both laboratory and field conditions to investigate energy leakage below 200 kHz.

A. Methods

The commercial echo sounder was evaluated in both the laboratory and in the field. For all tests in both environments, the detection range setting applied in the software on the surface unit of the sonar was 200 m, the most likely candidate mode for the final active monitoring system. To measure the underwater acoustic signal transmitted by the sonar, a hydrophone with a built-in 26-dB preamplifier (RESON TC4014-5) was used. The output from the hydrophone was connected to a voltage preamplifier with a built-in band-pass filter (RESON EC6068), which filtered-out signals below 1 Hz and above 750 kHz without supplying any additional gain. The filtered signal was then connected to a commercial data acquisition card (Model PXIe-6124, National Instruments [NI], Austin, TX) housed in an NI chassis (Model PXIe-1073) and connected to a computer running the Microsoft Windows 7 operating system. The NI data acquisition card featured a 16-bit analog-to-digital converter, and the data were collected at the maximum sampling rate of 4 MHz. The data acquisition card was controlled by a MATLAB program (The MathWorks, Inc., Natick, MA) written for these tests. The program was set up to record 6 continuous seconds per file. After the data were collected, a separate MATLAB program was created to process the waveforms by converting the waveform to physical pressure units, isolating individual pulses, performing a fast Fourier transform to calculate the sound pressure level (SPL) using Welch's method with a Hanning window (8192 data points per window), 50% overlap, and a 305-Hz bandwidth to calculate the power spectrum density (PSD). The hydrophone and data acquisition system were previously calibrated in a water test tank lined with anechoic material [18].

The sonar was first evaluated in a large elongated oval laboratory tank approximately 7 m long × 3 m wide × 2 m deep. The sonar head was situated at one end of the tank at the middle of the water column oriented along the central axis of the tank. The hydrophone was located in line with the sonar head approximately 3.5 m away (Fig. 3).

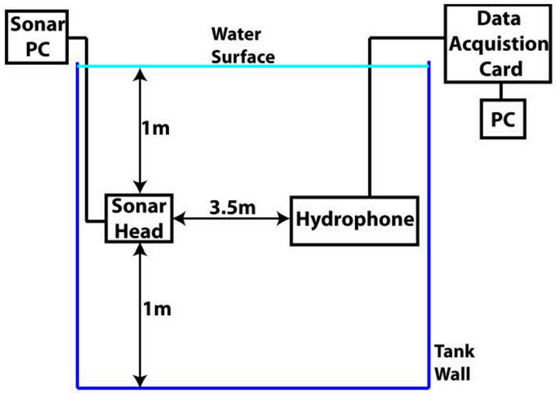

Figure 3. Experimental setup for evaluating the frequency content of active sonar in a laboratory tank (dimensions not to scale).

The sonar was then evaluated in the field, on the Columbia River at river kilometer 336.5, near Richland, WA. The sonar head was deployed at the middle of the water column from a boat dock at a location where the river was approximately 6 m deep. The hydrophone and data acquisition system were deployed from a boat, with the hydrophone located 13.5 m from the sonar head (Fig. 4).

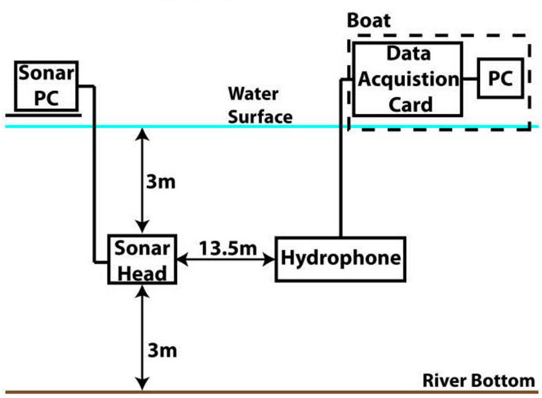

Figure 4. Experimental setup for evaluating the frequency content of active sonar on the Columbia River near Richland, WA.

B. Results and Discussion

The waveforms collected under the laboratory conditions were processed to identify individual sonar pulses (Fig. 5). Each pulse was slightly overlapped with reflections from the water surface and the sides of the tank (Fig. 5b). The SPL and PSD plots (Fig. 6) show that in addition to the primary peak at 200 kHz there was a secondary peak at approximately 90 kHz. This secondary peak had an amplitude of 125 dB at 3.5 m, which was approximately 51 dB less than the amplitude of the primary peak.

The waveforms collected in the field conditions were also processed to identify individual sonar pulses (Fig. 7). At 13.5 m from the sonar head, the reflections from the bottom and surface do not quite overlap (Fig. 7b). The SPL and PSD plots (Fig. 8) of the field measurements confirm a secondary peak at approximately 90 kHz. The amplitude of the secondary peak was about 118 dB at 13.5 m, which was about 47 dB less than the primary peak.

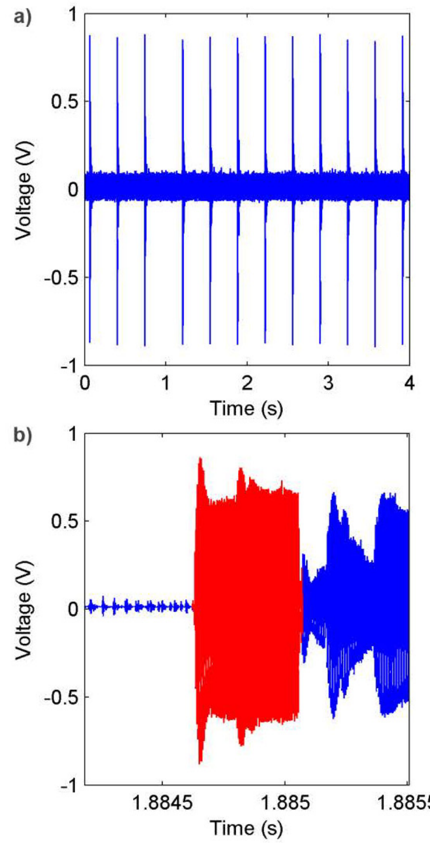

Figure 5. Original waveform collected using a hydrophone at 3.5 m from the sonar head in a laboratory tank. (a) Multiple pulses; (b) single pulse.

Assuming spherical spreading of the acoustic signal, the 90-kHz secondary peak in the results from the field testing had an amplitude of approximately 140 dB at 1 m. Using a 10% bandwidth, we integrated the power spectrum density of noise measurements performed at the proposed turbine site in Admiralty Inlet and determined that the 90-kHz sonar leakage must travel 72.0 m through saltwater before it is attenuated to the levels of the background noise.

Based on audiograms measured by [17], at 90 kHz the hearing threshold of killer whales is 70 dB. This indicates that killer whales would be able to hear the secondary sonar signal at 90 kHz. Although the killer whales would be able to hear this signal, [19] indicates that the amplitude of the secondary sonar signal does not exceed the threshold for potential injuries, which occurs at an SPL of 230 dB.

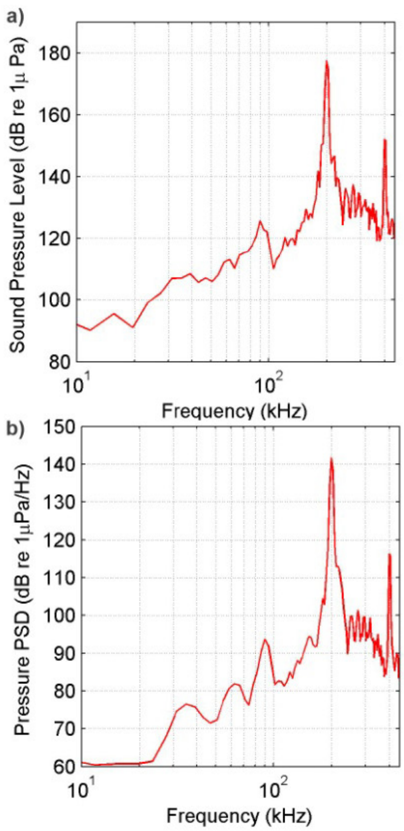

Figure 6. Sound pressure level and power spectrum density of the transmitted signal at 3.5 m from the sonar head in a laboratory tank. (a) Sound pressure level; (b) power spectrum density.

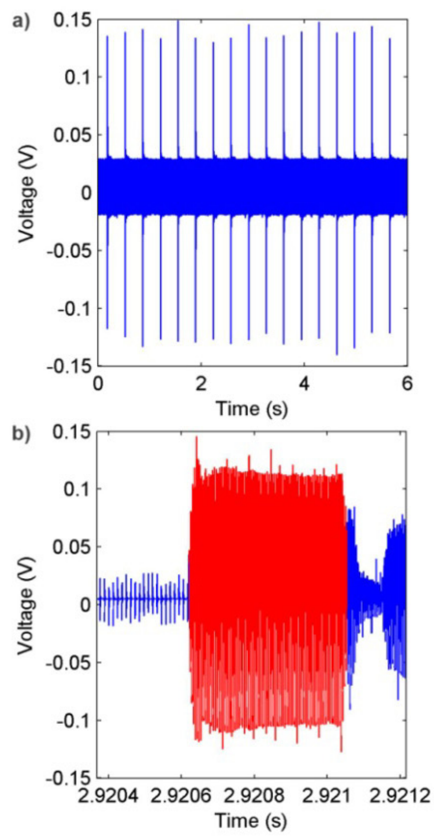

Figure 7. Original waveform collected using a hydrophone at 13.5 m from the sonar head on the Columbia River. (a) Multiple pulses; (b) single pulse.

IV. Conclusions

Target strength of an adult killer whale was modeled at a frequency of 67 kHz by assuming that a killer whale shares similar morphological structure with a bottlenose dolphin. The TS of killer whales at higher frequencies can be modeled using several methods. We are processing echograms of killer whales recorded by a sonar operating at 200 kHz in Puget Sound to provide direct validation data for the modeled results.

Direct measurements were performed on the frequency contents of a commercial multi-beam sonar in both laboratory and field conditions. Preliminary results show that potential leakage at a frequency of 90–95 kHz is above the hearing threshold of killer whales but below the threshold for potential injuries. Active sonars of two other vendors are being evaluated. In addition, we are investigating the effect of the potential energy leakage at lower frequencies on behavior of killer whales.

Acknowledgment

For their help with this study, the authors thank Brian Polagye, Jim Thompson, and Chris Bassett (University of Washington); Brandon Southall (SEA, Inc.); Jason Wood (Sea Mammal Research Institute, University of St. Andrews); and Tylor Abel, Charlie Brandt, Andrea Copping, Andrea Currie, Michele Halvorsen, Shari Matzner, Gene Ploskey, Matt Taubman, and Ning Zhou (Pacific Northwest National Laboratory [PNNL]). The study was conducted at PNNL, which is operated by Battelle for the U.S. Department of Energy.

References

[1] G. A. McMichael, M. B. Eppard, T. J. Carlson, J. A. Carter, B. D. Ebberts, R. S. Brown, M. Weiland, G. R. Ploskey, R. A. Harnish, and Z. D. Deng, "The Juvenile Salmon Acoustic Telemetry System: a new tool," Fisheries, vol. 35, no. 1, pp. 9–22, 2010.

[2] M. A. Weiland, Z. D. Deng, T. A. Seim, B. L. LaMarche, E. Y. Choi, T. Fu, T. J. Carlson, A. I. Thronas, and M. B. Eppard, "A cabled acoustic telemetry system for detecting and tracking juvenile salmon: part 1. engineering design and instrumentation," Sensors, vol. 11, no. 6, pp. 5645–5660, 2011.

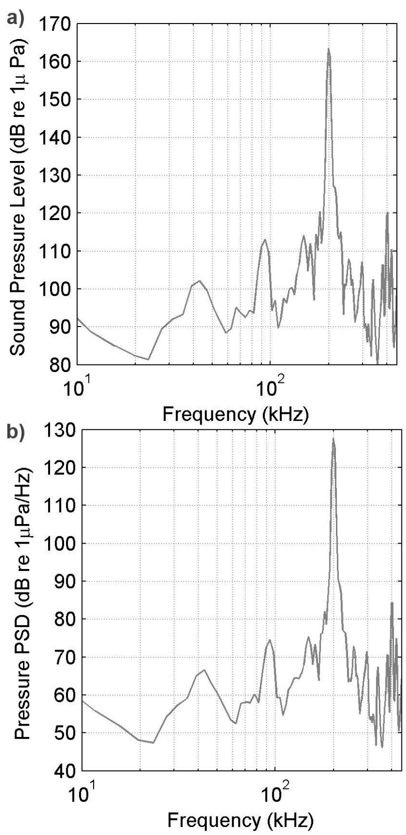

Figure 8. Sound pressure level and power spectrum density of the transmitted signal at 13.5 m from the sonar head on the Columbia River. (a) Sound pressure level; (b) power spectrum density.

[3] Z. D. Deng, M. A. Weiland, T. Fu, T. A. Seim, B. L. LaMarche, E. Y. Choi, T. J. Carlson, and M. B. Eppard, "A cabled acoustic telemetry system for detecting and tracking juvenile salmon: part 2. three-dimensional tracking and passage outcomes," Sensors, vol. 11, no. 6, pp. 5661–5676. 2011.

[4] W.W.L. Au, "Acoustic reflectivity of a dolphin," J. Acoust. Soc. Am., vol. 99, pp. 3844–3848, 1996.

[5] R. H. Love, "Dorsal-aspect target strength of an individual fish," J. Acoust. Soc. Am., vol. 49, pp. 816–823, 1971.

[6] D. B. Reeder and T. K. Stanton, "Acoustic scattering by axisymmetric finite-length bodies: an extension of a two-dimensional conformal mapping method," J. Acoust. Soc. Am., vol. 116, pp. 729–746, 2004.

[7] D. T. DiPerna and T. K. Stanton, "Sound scattering by cylinders of noncircular cross section: a conformal mapping approach,'' J. Acoust. Soc. Am., vol. 96, pp. 3064–3079, 1994.

[8] D. B. Reeder, J. M. Jech, and T. K. Stanton, "Broadband acoustic backscatter and high-resolution morphology of fish: measurement and modeling," J. Acoust. Soc. Am., vol. 116, pp. 747–761, 2004.

[9] K. G. Foote, "Rather-high-frequency sound scattering by swimbladdered fish," J. Acoust. Soc. Am., vol. 78, pp. 688–700, 1980.

[10] C. S. Clay, "Low-resolution acoustic scattering models: fluid-filled cylinders and fish with swimbladders," J. Acoust. Soc. Am., vol. 89, pp. 2168–2179, 1991.

[11] T. K. Stanton, "Sound scattering by cylinders of finite length. III. deformed cylinders," J. Acoust. Soc. Am., vol. 86, pp. 691–705, 1989.

[12] C. S. Clay and J. K. Horne, "Acoustic models of fish: the Atlantic cod (Gadus morhua),'' J. Acoust. Soc. Am., vol. 96, pp. 1661–1668.

[13] M. Born and E. Wolf Principles of Optics, Cambridge Univ. Press , 1999

[14] R. J. Urick, Principles of Underwater Sound for Engineers. New York: McGraw-Hill, 1983.

[15] S. H. Ridgeway and R. Howard, "Dolphin lung collapse and intramuscular circulation during free dive," Science, vol. 206, pp. 1182–1183, 1979.

[16] J. H. Miller and D. C. Potter, "Active high frequency phased-array sonar for whale ship strike avoidance: target strength measurements," OCEANS 2001, vol. 4, pp. 2104–2107. Piscataway, NJ: Institute of Electrical and Electronic Engineers, 2001.

[17] M. D. Szymanski, D. E. Bain, K. Kiehl, S. Pennington, S. Wong, and K. R. Henry, Killer whale (Orcinus orca) hearing: Auditory brainstem response and behavioral audiograms. J. Acoust. Soc. Am. 106, 1134–1141, 1999

[18] Z. Deng, M. A. Weiland, T. Fu, T. A. Seim, B. L. LaMarche, E. Y. Choi, T. J. Carlson, and M. B. Eppard, "Design and instrumentation of a measurement and calibration system for an acoustic telemetry system," Sensors, vol. 10, no. 4, pp. 3090--3099, 2011.

[19] B. L. Southall, A. E. Bowles, W. T. Ellison, J. J. Finneran, R. L. Gentry, C. R. Greene Jr., D. Kastak, D. R. Ketten, J. H. Miller, P. E. Nachtigall, W. J. Richardson, J. A. Thomas, and P. L. Tyack, "Marine mammal noise exposure criteria: initial scientific recommendations," Aquatic Mammals, vol. 33, no. 4, pp. 411–522, 2007.

Appendix C

Acoustic Environment of Admiralty Inlet: Broadband Noise Measurements

Acoustic Environment of Admiralty Inlet: Broadband Noise Measurements

Jinshan Xu, Z Daniel Deng*, Jayson J Martinez, Thomas J Carlson,
Joshua R Myers, Mark A Weiland, Mark E Jones
Pacific Northwest National Laboratory, PO Box 999, Richland, USA
* Author to whom correspondence should be addressed. Email: zhiqun.deng@pnnl.gov

Abstract—**Admiralty Inlet has been selected as a potential tidal energy site. It is located near shipping lanes, is a highly variable acoustic environment, and is frequented by the endangered southern resident killer whale (SRKW). Resolving environmental impacts is the first step to receiving approval to deploy tidal turbines at Admiralty Inlet. Of particular concern is the potential for blade strike or other negative interactions between the SRKW and the tidal turbine. A variety of technologies including passive and active monitoring systems are being considered as potential tools to determine the presence of SRKW in the vicinity of the turbines. Broadband noise level measurements are critical for determining design and operational specifications of ocean energy capture technologies. Acoustic environment data at the proposed site was acquired at different depths using a cabled vertical line array (VLA) with four calibrated hydrophones. The power spectrum density of the sound pressure level (SPL) was estimated using the fast Fourier transform. This study describes the first broadband SPL measurements for this site at different depths with frequencies ranging from 10 kHz to 480 kHz in combination with other information. To understand the SPL caused by bedload transport, three different pressure sensors with temperature and conductivity were also assembled on the VLA to measure the conditions at the hydrophone deployment depth. The broadband SPL levels at frequency ranges of 3 kHz to 7 kHz as a function of depth were estimated. Only the hydrophone at an average depth of 40 m showed the strong dependence of SPL with distance from the bottom, which was possibly caused by the cobbles shifting on the seabed. Automatic Identification System data were also studied to understand the influence of ship traffic on SPL measurements.**

Keywords-underwater acoustics; noise measurement; sound propagation; Tidal power

I. INTRODUCTION

Underwater ambient noise research began during World War II because of availability of calibrated instruments and a critical need to understand the performance of active/passive sonar systems. References [1] and [2] summarized most of the wartime research. The classic paper by [3] was notable, as it supplied a graphical or schematic spectrum of omnidirectional noise levels versus frequency from sources including wind, rainfall, shipping, and biota. The growth of the offshore (wind, wave, tidal) renewable energy industry in recent years has focused concern about the potential impact of a variety of machine factors, including noise, on marine biota.

Admiralty Inlet in northern Puget Sound has been selected by Snohomish County Public Utility District as a pilot site for the deployment of two OpenHydro hydrokinetic turbines because of its strong tidal current. Puget Sound is a large, fjordal system occupied by a variety of commercial and recreationally important species, and is home to an endangered population of orca — the southern resident killer whale (SRKW). Quantifying and resolving potential environmental impacts is a first step to receiving approval to deploy these turbines in Admiralty Inlet. Of particular concern is the potential for blade strike or other negative interactions between the SRKW and tidal devices. A variety of technologies including passive and active monitoring systems are being considered as potential tools to determine the presence of SRKW in the vicinity of the proposed test sites. A passive monitoring system is being developed by modifying an energy-based juvenile salmon acoustic telemetry system [4-6]. The active monitoring system focuses on a system that has no energy leakage at lower frequencies affecting the behavior of SRKW. Broadband ambient and turbine-system noise level measurements are therefore critical for determining design and operation specifications.

A team led by Jim Thomson and Brian Polagye from the Northwest National Marine Renewable Energy Center have been using a variety of instruments to collect ambient acoustic data in Admiralty Inlet during the last two years [7]. However, these data covered frequencies up to only 40 kHz. For our proposed passive and active monitoring systems, the possible frequency range extends up to 200 kHz, which requires measurements at higher frequencies.

In this paper, we describe the broadband sound pressure level (SPL) measurements for this site at different depths with frequency ranging from 1 kHz to 480 kHz in combination with other information.

II. EXPERIMENT AND INSTRUMENTS

A. Hydrophones

A cabled vertical line array (VLA) with four calibrated hydrophones was deployed from a ship platform (*R/V*

This study is funded by the U.S. Department of Energy, Office of Energy Efficiency and Renewable Energy, Wind and Water Power Program.

Robertson, Applied Physics Laboratory, University of Washington) at a water depth around 60 m approximately 1 km offshore of Fort Casey in Admiralty Inlet on February 11, 2011. The four calibrated hydrophones were Reson TC4034, TC4014, TC4040, and TC4034 with different frequency coverage ranging from 1 Hz up to 480 kHz and sensitivities from −186 dB to −226 dB re 1 V/µPa (Fig. 1). Table I summarizes the deployment depths, specifications, and sampling rate of the different sensors. The hydrophones were calibrated in a water test tank lined with anechoic material [9].

B. Data Acquisition Systems

The sound pressure data were recorded using a National Instruments (NI) PXIe-6124 with a 16-bit analog to digital converter (A/D) and an NI PXI-6110 with 12 bits A/D at two different sampling rates of 500 kHz and 2.5 MHz [6]. A total of 130 data sets were collected within 2.5-hour time windows at different depths. PXIe-6124 was set up to collect 60 seconds of data at the 500-kHz sampling rate and 12 seconds of data at the 2.5-MHz sampling rate with input voltage range of ± 1 V. The PXI-6110 was set up to collect 32 seconds of data at the 500-kHz sampling rate and 6.4 seconds at the 2.5-MHz sampling rate with input voltage range of ± 0.5 V.

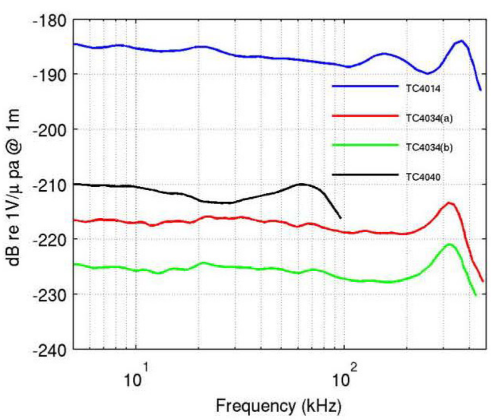

Figure 1. Sensitivity curves of different hydrophones deployed for the survey on February 11, 2011.

TABLE I. VERTICAL LINE ARRAY INSTRUMENTS

Instrument	Mean Depth (m)	Specification	NI Board	Sampling Rate
TC4034	17	Frequency range 1 Hz–470 kHz; Sensitivity −218 dB ±3 dB re 1 V/µPa	NI6110 (12 bits A/D)	0.5/2.5 MHz
TC4014	22	Frequency range 15Hz–480 kHz; Sensitivity −186 dB ±3 dB re 1 V/µPa	NI6124 (16 bits A/D)	0.5/2.5 MHz
TC4040	36	Frequency range 15 Hz–120 kHz; Sensitivity − 206dB ±3 dB re 1 V/µPa	NI6110 (12 bits A/D)	0.5/2.5 MHz
TC4034	40	Frequency range 1 Hz–470 kHz; Sensitivity −218 dB ±3 dB re 1 V/µPa	NI6124 (16 bits A/D)	0.5/2.5 MHz
SB39	22.7	Temperature/pressure	N/A	0.33 Hz
SB19	41	Temperature/pressure/ conductivity	N/A	0.1 Hz

The two data acquisition boards have different self-noise floors, which is a function of sampling rate and input voltage range. The PXIe-6124 has a noise floor of −147 dB re 1 V/rtHz at the 2.5-MHz sampling rate with input voltage range of ± 1 V and −140 dB re 1 V/rtHz at the 500-KHz sampling rate with input voltage range of ± 1V. The noise floor of the PXI-6110 is −133 dB re 1 V/rtHz at the 500-KHz sampling rate with input voltage range of ± 0.5 V and −140 dB re 1 V/rtHz at the 2.5-MHz sampling rate with input voltage range of ± 0.5 V. The self-noise floors of the data acquisition systems determine the lowest SPL the particular hydrophones could measure, which will be discussed in the next section.

There were two known active acoustic sources: an acoustic modem signal at 10 kHz and a sinusoidal signal at 416 kHz with source level 156 dB re 1 µPa at 1 m transmitted by a TC4034 hydrophone. These transmissions were both low duty cycle, and each transmission was recorded with time-stamps. The vessel engine and all acoustic instruments including echo sounder and acoustic Doppler current profiler were turned off during the acoustic survey to reduce any possible interference with SPL measurements. The vessel was drifting free at an average speed of 3 knots (1.54 m/second) throughout the acoustic survey period due to the strong current at the survey site, with maximum currents exceeding 3 m/second. Every VLA deployment lasted about 30 minutes. Commercial shipping and ferry vessel traffic were found to be the most significant contributors to ambient noise levels at this site. Post-processed data from the Automatic Identification System (AIS), which tracks ship movement, was used to determine the location of ships during each recording.

Cobbles shifting on the seabed from strong tidal currents can create noise ranging from 1 kHz to 10 kHz [8]. Three different pressure sensors with temperature (Seabird Microtemp 39) and conductivity (Seabird 19) were deployed on the vertical line array (Table 1) to measure the conditions at the hydrophone deployment depth to help understand the SPL caused by this bedload transport and the background sound speed profile. The broadband SPL levels at frequency ranges of 1 kHz to 20 kHz as a function of depth were estimated.

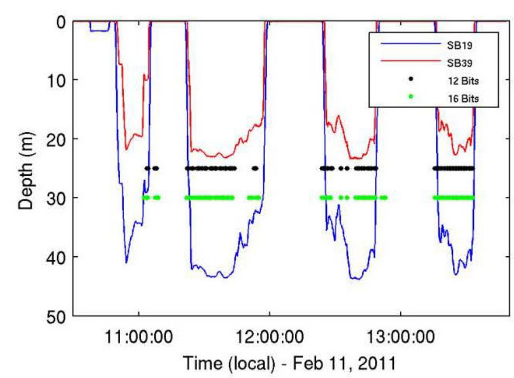

Figure 2. Seabird depth sensor measurements and hydrophone acoustic sampling time information. Blue line: depth measured by Seabird 19; red line: depth measured by Seabird 39; black dots: acoustic sampling time from NI6110(12bits A/D); green dots: acoustic sampling time from NI6124(16 bits A/D)

Fig. 2 shows the depth measurement of Seabird 39 and 19 during the entire February 11 acoustic survey. The acoustic sampling points from two different data acquisition systems are also plotted to display the time information of acoustic measurement. The depths of VLA varied among the four deployments (Fig. 3) during the 2-hour time windows due to the strong current and drifting of the research vessel.

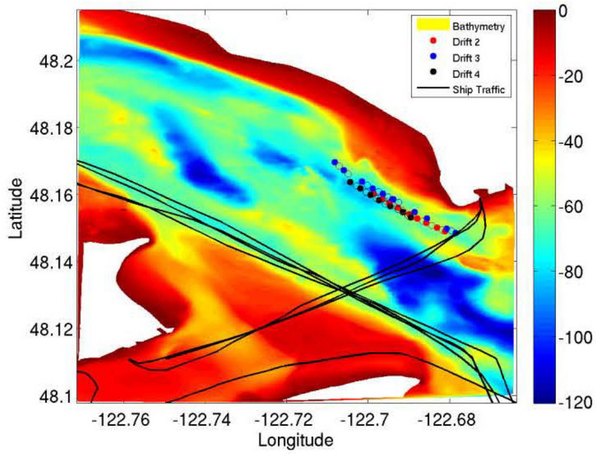

Figure 3. The bathymetry map of the North Admiralty Inlet overlapped with acoustic survey site locations and ship trafic from 1100 hours to 1330 hours on February 11, 2011. The dots and circles indicate the acoustic sampling location points from different Daqs: the circles are from NI6110 with 12 bits A/D; the dots are from NI6124 with 16 bits A/D. The different colors indicate the different drifts.

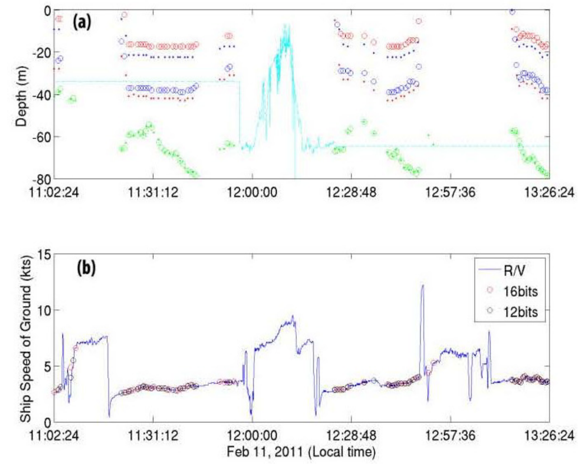

Figure 4. Upper panel: red circles: TC4034/ NI6110; blue circles: TC4040/NI6110; blue dots: TC4014/NI6124; red dots: TC4034/NI6124; green circles: local water depth. Lower panel: research vessel speed of ground.

III. Data Analysis

Some acoustics data were recorded when the hydrophones were still on deck or being deployed/recovered, so the first step in processing the data was to use the depth information of hydrophone and the speed of the research vessel to remove those non-representative data. We used only those acoustic measurements that came from a depth greater than 6 m and while the vessel drifting speed was less than 5 knots. Fig. 4 shows the combined information of hydrophone depths and research vessel speed.

Welch's method was used to process all the data with a fast Fourier transform length of 8192, Hanning window, and 50% overlap for the averaging, which corresponds to an approximate 0.003-second time window of data. The frequency bin size was approximately 305 Hz. The acoustic modem (10-kHz signal) was operating constantly during the survey. However, the 10-kHz signal was a narrowband signal, so it was not necessary to remove it for noise level estimation in the wide frequency band.

One 60-second data set was contaminated by the SB19 water pump. Another 60-second dataset and one 12-second dataset contained possible vocal sounds (clicks) from a marine mammal, with center frequency at 50-kHz broadband signals. All three data sets were removed from SPL calculations.

IV. Results and Discussion

Fig. 5 shows the sound pressure level power spectral density (PSD) measured at different depths. The depth ranged from 17 m to 40 m below the sea surface, and PSD varied from 10 to 20 dB at different frequency bands. The TC4034s did not measure the true noise levels at most frequencies due to its very low sensitivity and high self-noise level, especially when the sound environment is relative quiet.

The broadband SPL levels at frequency ranges of 3 kHz to 7 kHz, as a function of depth, were estimated for all four depths (Fig. 6). Only the result from the deepest deployed hydrophone at an average depth of 40 m showed the strong influence of bedload transport on SPL. However, it is difficult to draw a conclusion because of insufficient data. Previous measurements in the same general location showed strong correlation between the broad SPL and average vertical current speed [7].

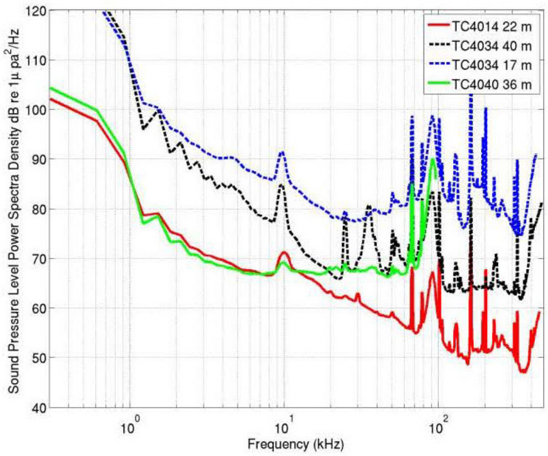

Figure 5. Frequency power spectral density of sound pressure level measured by different hydrophones at different depths. Spectrum level is the averaged result for about 2 hours duration.

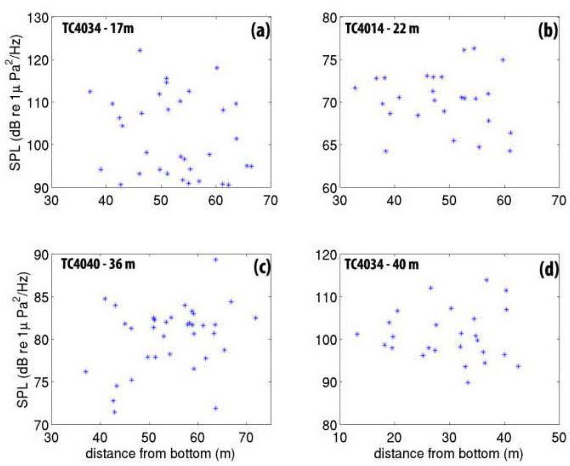

Figure 6. Averaged power spectra density of sound pressure level in the frequency band from 3-7 kHz as function of the distance from the bottom of four different hydrophones.

The data acquisition system with the TC4014 and PXIe-6124 had low self noise and produced the best results. For 60-second duration measurements at the 500-kHz sampling rate (Fig. 7a), the SPL of drift 4 was different from those of drifts 2 and 3 in the frequency range of 500 Hz to 20 kHz, and drifts 2 and 3 had narrowband frequency components of 650 Hz, 1.25 kHz and 1.75 kHz. For 12-second duration measurements at the 2.5-MHz sampling rate (Fig. 7b), the SPL of drift 4 (black) was different from those of drifts 2 and 3 in the frequency range of 5 kHz to 50 kHz, and it has broadband sound pressure level increasing up to 68 dB.

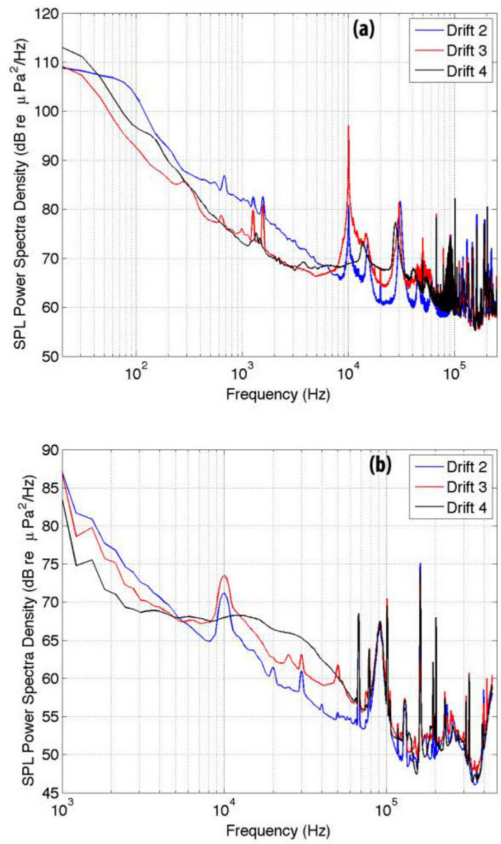

Figure 7. Sound pressure level power spectra density measured by TC4014 from different drifts. (a) 60-second duration at sampling rate of 500 kHz; (b) 12-second duration at sampling rate of 2.5 MHz.

The AIS data were divided into separate time periods relative to the sampling drift times to better understand the effects of ship traffic on these measurements. Fig. 8 shows the AIS data combined with acoustic survey location points for drifts 2, 3, and 4. In drift 2, three vessels were recorded by the AIS; one of them was a ferry crossing from south to north. During drift 3, four vessels were recorded by AIS; one was a ferry. During drift 4, there was only a ferry preparing to leave for Port Townsend. Therefore, the SPL measurements during drifts 2 and 3 most likely contained the shipping traffic signal. Drift 4 data could be the least affected by the shipping traffic.

The ambient noise refers to the noise that remains after all easily identifiable sound sources are eliminated, and it is treated as the resident acoustic field in the ocean. For instance, the presence of many ships randomly distributed over the ocean surface results in a component of ambient noise attributed to distant shipping traffic. In general, the distant ship traffic mainly contributes to the underwater noise in the frequency band of 50-500 Hz [3], since the attenuations of sound at these frequencies in the deep ocean is relatively small.

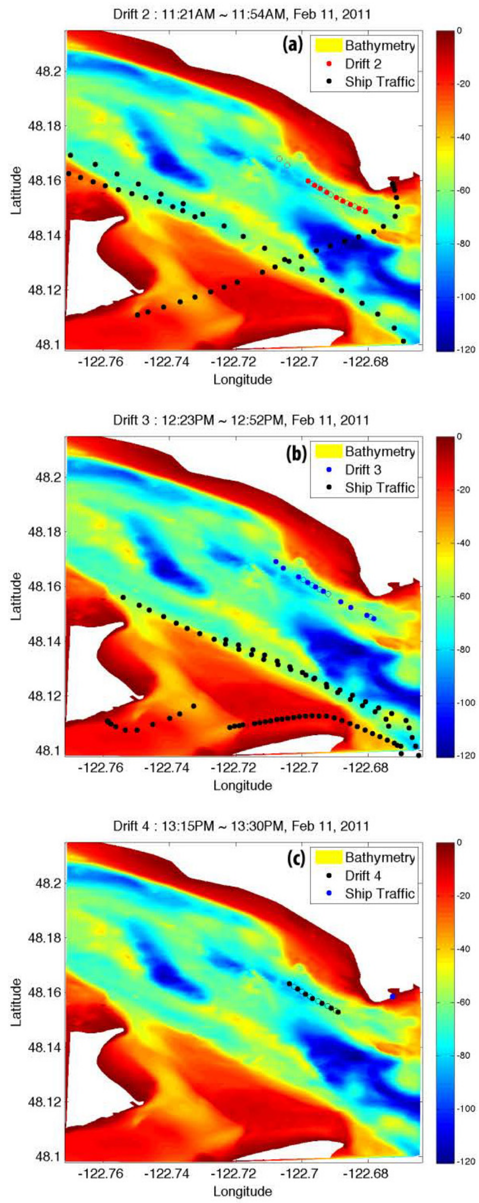

Figure 8. AIS data recorded shipping trafic from different drifts overlapped with bathymetry data. (a): Drift 2 – 11:21 AM to 11:54 AM; red circles are acoustic sampling location points from NI6124 with sampling rate of 2.5MHz; the red dots are acoustic smapling location points from NI6110 with sampling rate of 500 kHz, black dots are shipping trafic points; (b): Drift 3 – 12:23 PM to 12:52 PM; blue dots are acoustic survey location points from NI6124 with sampling rate of 2.5 MHz, blue circles are acoustic survey location points from NI 6110 with sampling rate of 500 kHz, black dots are shipping trafic points; (c) Drift 4 – 13:15 PM to 13:30 PM; the black dots are acoustic survey location points from NI 6124 with sampling rate of 2.5 MHz, the black circles are acoustic survey location points from NI6110 with sampling rate of 500 kHz, the blue dots are shipping trafic points(ferry).

However, if the noise produced by a single nearby ship is easily identified, it is treated as an acoustic signal instead of as a part of ambient noise [10]. AIS data are especially useful in processing the sound pressure data and understanding the sound pressure increases caused by this kind of shipping traffic. For example, the discrete acoustic signal signature at frequencies of 500 Hz to 2 kHz of drifts 2 and 3 (Fig. 7a) were from the shipping traffic identified from AIS.

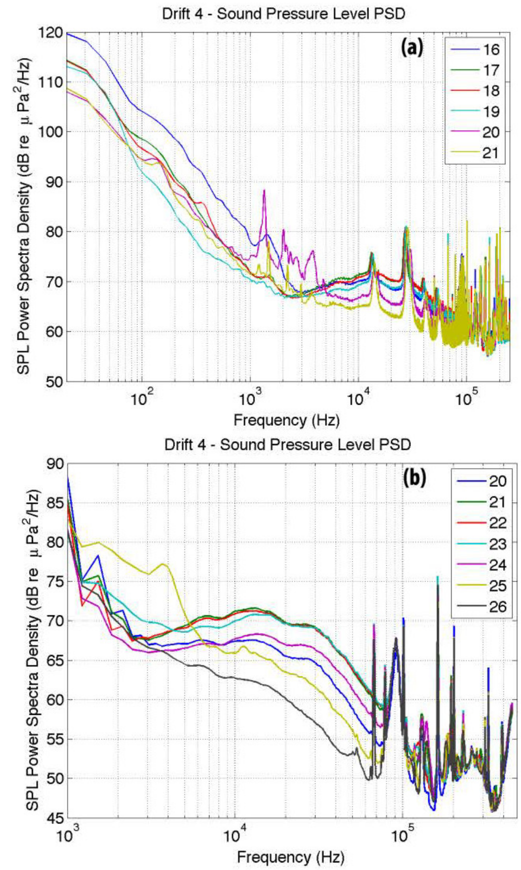

Figure 9. Power spectra density of SPL measurement during drift 4. (a) SPL from the 60-second duration at sampling rate of 500 kHz; (b) SPL from the 12–second duration at sampling rate of 2.5 MHz. Numbers in the legend reflect the numbers of the files, which were recorded chronologically..

The broadband acoustic signal from 5 kHz to 50 kHz of drift 4 (Fig. 7b) may be due to seabed sediment movement; the research vessel drifting speed was about 4 knots during this period, which was almost the strongest current during that time window. SPL estimations from individual data sets of drift 4 also show the strong time-dependence of SPL in the frequency band between 3 kHz and 60 kHz, possibly caused by the bedload transportation with strong current during the survey.

V. CONCLUSION

Broadband SPL measurements at different depths with frequency ranging from 1 kHz to 480 kHz were performed at Admiralty Inlet in northern Puget Sound, a potential test site for the deployment of hydrokinetic turbines. Three different pressure sensors with temperature and conductivity were also assembled on the VLA to measure the conditions at the hydrophone deployment depth to understand the SPL caused by bedload transportation. The broadband SPL levels at frequency ranges of 1 kHz to 20 kHz, as function of depth, were estimated.

The SPL measurement from TC4014 was studied in detail in combination with other information from Seabird sensor units and AIS data. The underwater noise level is affected by natural and anthropogenic sources. The nearby shipping traffic had significant SPL signatures in the frequency ranges from 500 Hz to 20 kHz. In addition, the bedload transport may have increased the broadband SPL in frequency ranging from 3 kHz to 60 kHz.

More broadband noise data sets have been collected from two recent trips using better hydrophones and data acquisitions systems. Data analysis is under way, and all results will be integrated to provide a better understanding of the broadband acoustic environment at the proposed test site for the deployment of hydrokinetic turbines.

Acknowledgment

For their help with this study, the authors thank Brian Polagye, Jim Thompson, and Chris Bassett (University of Washington); Brandon Southall (SEA, Inc.); Jason Wood (Sea Mammal Research Institute, University of St. Andrews); and Tylor Abel, Charlie Brandt, Andrea Copping, Andrea Currie, Michele Halvorsen, Shari Matzner, Bob Mueller, Gene Ploskey, Matt Taubman, and Ning Zhou (Pacific Northwest National Laboratory [PNNL]). The study was conducted at PNNL, which is operated by Battelle for the U.S. Department of Energy.

References

[1] V. O. Knudsen, R. S. Alford, and J. W. Emling, "Underwater ambient noise," J. Marine Res., vol. 7, pp. 410–429, 1948.

[2] R. J. Urick and A. W. Pryce, A Summary of Underwater Acoustic Data, Part V, Background Noise," Office of Naval Research, Arlington, VA, 1954.

[3] G. Wenz, "Acoustic ambient noise in the ocean: spectra and sources,"J. Acoust. Soc. Am., vol. 34, no. 12, pp. 1936–1956, 1962.

[4] G. A. McMichael, M. B. Eppard, T. J. Carlson, J. A. Carter, B. D. Ebberts, R. S. Brown, M. Weiland, G. R. Ploskey, R. A. Harnish, and Z. D. Deng, "The Juvenile Salmon Acoustic Telemetry System: a new tool," Fisheries, vol. 35, no. 1, pp. 9–22, 2010.

[5] M. A. Weiland, Z. D. Deng, T. A. Seim, B. L. LaMarche, E. Y. Choi, T. Fu, T. J. Carlson, A. I. Thronas, and M. B. Eppard, "A cabled acoustic telemetry system for detecting and tracking juvenile salmon: part 1. engineering design and instrumentation," Sensors, vol. 11, no. 6, pp. 5645–5660, 2011.

[6] Z. D. Deng, M. A. Weiland, T. Fu, T. A. Seim, B. L. LaMarche, E. Y. Choi, T. J. Carlson, and M. B. Eppard, "A cabled acoustic telemetry system for detecting and tracking juvenile salmon: part 2. three-dimensional tracking and passage outcomes," Sensors, vol. 11, no. 6, pp. 5661–5676. 2011.

[7] C. Bassett, J. Thomson, and B. Polagye, "Characteristics of underwater ambient noise at a proposed tidal energy site in Puget Sound," Oceans 2010,. Piscataway, NJ: Institute of Electrical and Electronic Engineers, 2010.

[8] T. Mason T. , D. Priestley, D.E. Reeve, "Measuring shingle sediment transport under waves using a passive acoustic technique," J. Acoust. Soc. Am.vol. 122, no. 2, pp. 737-745, August 2007.

[9] Z. Deng, M. A. Weiland, T. J. Carlson, and M. B. Eppard, "Design and instrumentation of a measurement and calibration system for an acoustic telemetry system," Sensors, vol. 10, no. 4, pp.3090–3099, doi:10.3390/s100403090, 2010.

[10] Burdic, W.S. "Underwater acoustic system analysis"; 2nd Ed, Penisula Publishing: Los Altos Hills, CA, USA, 1990.

Pacific Northwest
NATIONAL LABORATORY

Proudly Operated by Battelle *Since 1965*

U.S. DEPARTMENT OF
ENERGY

902 Battelle Boulevard
P.O. Box 999
Richland, WA 99352
1-888-375-PNNL (7665)
www.pnnl.gov